OULUN YLIOPISTO
UNIVERSITY of OULU
DEGREE PROGRAMME IN WIRELESS COMMUNICATIONS ENGINEERING

MASTER'S THESIS

DECENTRALIZED COORDINATED TRANSCEIVER DESIGN WITH LARGE ANTENNA ARRAYS

Author	Hossein A.Moghaddam
Supervisor	Docent Antti Tölli
Second Supervisor	Docent Premanandana Rajatheva

September, 2013

A.Moghaddam A. (2013) Decentralized Coordinated Transceiver Design with Large Antenna Arrays. University of Oulu, Department of Communications Engineering, Master's Degree Program in Wireless Communications Engineering. Master's thesis, 61 p.

ABSTRACT

The benefits of MIMO technology have made it a solution for the present and future wireless networking demands. Increasing the number of antennas is an intuitive approach for boosting the network capacity; however, processing load and implementation limitations put a practical bound on this goal. Recently a solution known as massive MIMO has shown that a very large antenna array at the base station can simplify the processing, in a way that even matched filter (MF) can be used for detection purpose.

The ultimate performance of massive MIMO can be achieved only under some optimistic assumptions about the channel and hardware deployment. In practice, there are some restrictions that do not allow the ultimate performance for a massive MIMO system. Under some realistic assumptions, an efficient use of all the resources becomes important in a way that the application of simple algorithms like MF and zero forcing (ZF) becomes questionable. Thus, in this thesis work, more efficient approach based on optimal minimum power beamforming is considered as the benchmark. The idea is to investigate the behavior of this algorithm and the performance differences with respect to some sub-optimal methods when the system dimensions grow large.

Two solutions for the minimum power beamforming are reviewed (SOCP and uplink-downlink duality). The solution that is on focus is based on the second order cone programming (SOCP). Intercell interference(ICI) plays a critical role in the SOCP algorithm as it couples the sub-problems at the base stations. Thus, a large dimension approximation for the optimal ICI, using random matrix theory tools, is derived which tackles both of the processing simplification and the backhaul exchange rate reduction goals. This approximation allows derivation of an approximated optimal intercell interference based on the channel statistics that results a procedure for decoupling the subproblems at base stations.

The comparison between the SOCP algorithm and the sub-optimal methods is carried out via simulation. The results show that the performance gap with respect to the sub-optimal methods grows when correlation between the antenna elements at the BS side increase. In a network simulation with 7 cell and 28 users, this gap remains significant even with 100 antennas at the BS side. These performance differences justify the application of more complex algorithms like SOCP for a MIMO system with a large antenna array when the practical restrictions are taken into account.

Keywords: Massive MIMO, Large antenna array, CoMP, Minimum power beamforming, second order cone, uplink-downlink duality, random matrix theory, large dimensions approximation, Pilot contamination, Imperfect CSI

TABLE OF CONTENTS

FOREWORD

The focus of the thesis work is further study of the theoretical foundations of Massive MIMO. The target is to see how beneficial is the cooperation between base stations, when the number of antennas grows large, up to a practical limit. This research work has been done as a part of METIS (Mobile and Wireless Communications Enablers for the Twenty-twenty Information Society) and CRUCIAL (Solutions for Capacity Crunch in Wireless Access with Flexible Architectures) projects at Center for wireless communication (CWC).

Here, I would like to gratefully acknowledge my supervisor Docent Antti Tölli and second supervisor Docent Premanandana Rajatheva, for their support and valuable hints and comments. I would like to thank Prof. Matti Latva-aho for giving me an opportunity to work in CWC. Finally, I am deeply grateful to my wife and my parents, all of whom provided endless and unconditional support throughout different stages of my life.

LIST OF ABBREVIATIONS AND SYMBOLS

$a_{b,i}$	Pass loss from base station b to user i
$\mathcal{B}_k$	Set of BSs that serves user k
$\mathcal{B}$	Set of all BSs
$\overline{\mathcal{B}_k}$	The Set complements to $\mathcal{B}_k$
$\mathbb{C}^n$	Complex space of n dimensions
$\mathbb{CN}(0, I)$	Circularly-symmetric complex normal distribution
d_k	Data symbol for user k
$E[x]$	Expected value of random variable x
$\mathbf{h}_i$	Channel vector of user i
$\mathbf{h}_{b,i}$	Channel vector from base station b to user i
$\breve{\mathbf{h}}_{ij}$	MMSE estimate of channel vector $\mathbf{h}_{ij}$
$\tilde{\mathbf{h}}_{ij}$	Error in MMSE estimate of channel vector $\mathbf{h}_{ij}$
$\mathbf{I}_{\mathrm{N_a}}$	$\mathrm{N_a} \times \mathrm{N_a}$ Identity matrix
$\Im[z]$	Imaginary part of complex number z
$\mathbf{K}_{ij}$	Correlation matrix of channel vector $\mathbf{h}_{ij}$
$limSup_n y_n$	limit superior of an infinite sequence of numbers.
$m_{\mathbf{\Sigma}_b}(z)$	The stieltjes transform of $\mathbf{\Sigma}_b$ at point z
$min(x, y)$	Minimum of x and y
N_{a}	Number of antennas at Base station
N_{u}	Number of users
N_{s}	Number of sub-carriers
N_{t}	Number of transmit antennas
N_{r}	Number of receive antennas
N_{c}	Number of cells
N_{ts}	Number of time slots
N_{B}	Number of base stations
N_0	Noise spectral density
$\mathbf{n}$	Noise vector
$p_{b,k}$	Downlink power assigned by base station b to user k
p_{out}	Outage probability
$\mathbb{R}^n$	Real space of n dimensions
$\Re[z]$	Real part of complex number z
$Supp(F)^c$	Complex space complementary to the support of F
$tr[\mathbf{X}]$	Trace of matrix $\mathbf{X}$
$\mathcal{U}_b$	Set that contains the users allocated to the b^{th} base station
$\overline{\mathcal{U}_b}$	The Set complements to $\mathcal{U}_b$
$\mathcal{U}$	Set of all users
$vec(\mathbf{A})$	Vectorizing operator that puts the columns of matrix $\mathbf{A}$ in a vector form.
$\mathbf{w}_k$	Beamforming vector for user k
$\mathbf{w}_{b,k}$	Beamforming vector for user k at base station b
$\mathbf{W}$	Matrix that contains all the beamforming vectors
$\hat{\mathbf{w}}_{b,k}$	Uplink detection vector for user k at base station b
$\mathbf{x}_k$	Precoded data vector for user k
$\mathbf{x}_{b,k}$	Precoded data vector for user k at base station b

$\mathbf{y}$	Received data vector
$\mathbf{1}_{Nu}$	A $Nu \times 1$ vector with all elements equal to one
$\|\mathbf{h}\|$	Norm 2 of vector $\mathbf{h}$
$\|\|\mathbf{A}\|\|$	Spectral norm of matrix $\mathbf{A}$
α	The parameter that defines distance between user groups
$\epsilon_{b,k}$	An optimization variable that presents ICI from b^{th} BS to k^{th} user
$\epsilon_{b,k}^{b}$	Local copy of $\epsilon_{b,k}$ at the b^{th} base station
γ_k	SINR of user k
λ_k	Uplink power allocation variable for k^{th} user
$\mathbf{\Sigma}_b$	A matrix that contains channel vectors from b^{th} base station to all users
$\mathbf{\Theta_{ij}}$	Covariance matrix of channel estimate $\breve{\mathbf{h}}_{ij}$
ρ	Signal to noise ratio
ρ_{t}	Effective training SNR

ADMM	Alternating direction method of multipliers
AWGN	Additive white Gaussian noise
BS	Base station
CoMP	Coordinated multi-point
CSI	Channel state information
CWC	Center for wireless communications
d.o.f	Degrees of freedom
e.s.d	Empirical spectral distribution
FDD	Frequency-division duplexing
i.i.d.	Independent and identically distributed
ICI	Intercell interference
IEEE	Institute of electrical and electronics engineers
LOS	Line of sight
LTE	Long term evolution
METIS	Mobile and wireless communications Enablers for the Twenty-twenty Inforn
MF	Matched filter
MIMO	Multiple input Multiple output
MMSE	Minimum mean square error
mW	Milliwatt
non-LOS	Non line of sight
Num	Number
p.d.f	Probability density function
QOS	Quality of service
RF	Radio frequency
RMT	Random matrix theory
RZF	Regularized zero forcing
SINR	Signal to interference and noise ratio
SNR	Signal to noise ratio
SOC	Second order cone
SOCP	Second-order cone programming
TDD	Time-division duplexing
TDMA	Time-division multiple-access

ULA	Uniform linear array
ZF	Zero forcing
3GPP	3rd generation partnership project

1. INTRODUCTION

MIMO technology is currently considered in 3GPP standard for LTE [1],[2]. The releases of 3GPP standard have allowed the application of MIMO technology with different limits. For example, release 10, which is known as LTE-Advanced, supports up to 8 independent spatial streams for spatial multiplexing. Also, users are allowed to have up to 4 antennas [2].

Multiple antennas provide diversity gain ($P_{out} \propto SNR^{-N_{\mathrm{t}}N_{\mathrm{r}}}$, where P_{out} is outage probability and $N_{\mathrm{t}}, N_{\mathrm{r}}$ are the number of transmit and receive antennas respectively) , N-fold receive and transmit beamforming gains [3]. Also under favorite channel conditions, multiple receive and transmit antennas provides an additional spatial dimension which results in a degree of freedom gain (Capacity $\propto min(N_{\mathrm{t}}, N_{\mathrm{r}})log(SNR)$ for high SNR) [3]. Multiple antennas at base station (BS) allow simultaneous communication with multiple users that are spatially separated. This scheme can be combined with multiuser diversity gain for achieving higher rate (resulted from user selection) [3].

However, the advantages of MIMO technology come with a cost. Generally increasing the number of antennas means increasing the number of RF chains and the processing load. There are some other drawbacks such as: the required implementation space for multiple antennas, the increased battery consumption due to the processing load of multi antennas at the user terminal and etc. [4]. Therefore, one might conclude that the number of antennas in a MIMO system is limited by the above mentioned drawbacks, but this is not the whole story.

Authors in [5] present the concepts of massive MIMO, where a base station with a large antenna array serves multiple users simultaneously, on the same frequency and time resources. In a massive MIMO system, a BS with 100 or even 1000 antennas might be considered [4]. This large number of antennas at the BS, not only provides some additional spatial d.o.f (degree of freedoms), but also it results in a reduction in the transmit power and the interference level. Moreover, when the dimensions of a MIMO system grow large, the results of random matrix theory can be applied [6]. According to the random matrix theory, when the dimensions of a matrix (with some mild assumptions on the statistics of the entries) grow large, the distribution of e.s.d (empirical spectral distribution) of the matrix becomes deterministic [6]. This predictable behavior allows some simplifications in processing, in a way that even matched filter can be applied for detection in an ideal scenario (these issues will be discussed in detail in Chapter 2).

From the perspective of hardware implementation, it must be noted that the power per antenna is proportional to $1/N_{\mathrm{t}}^2$. Thus, the power amplifier for each antenna element becomes low power units, in the order of mW [4]. This allows using "small active antenna units which are plugged into an (optical) field-bus", thus bulky coaxial cables and high power amplifiers can be removed [4]. In addition, application of millimeter-wave frequencies for massive MIMO has been considered recently which allows shrinking the size of antenna array.

However, the ultimate performance of massive MIMO can be achieved only under some optimistic assumptions about the channel and hardware deployment. In practice, the propagation medium restricts the number of d.o.f that is achievable. Also some other considerations such as: implementing a large number of antennas in a given

space and the problems with correlation and coupling, hardware impairments etc, do not allow achieving the ideal performance for a massive MIMO system. Therefore, some more realistic assumptions must be considered when dealing with a massive MIMO system. Authors in [7] and [8] provide channel measurements for the cases with a large antenna array which confirms the above mentioned limitations.

Switching from an optimistic view to a more realistic one, opens a space for the application of optimal beamforming/detection methods to the massive MIMO scenario. One such approaches is CoMP (coordinated multi-point) which is already considered in 3GPP standard. CoMP allows cooperation between nodes for delivering services to users which results in a reduction in transmit power and interference level [9]. In order to fulfill this coordination, the base stations must share some information. Depending on what kind of information is shared among the nodes, CoMP can be divided in two categories: the first one is joint processing that obliged the user's data to be shared between the coordinated nodes. Then several nodes might jointly serve the user. The second type is coordinated beamforming/scheduling, where the user's data is just available in its serving node and decisions about beamforming/scheduling are made jointly by sharing some information like CSI (channel state information) [10],[11].

The coordination of the nodes based on the joint processing, which is also known as network MIMO [12], mitigates the interference problem and provides a huge capacity gain for the network. Nevertheless, sharing the user's data and CSI between the nodes make the practical implementation difficult, especially when dealing with a large number of users scattered in a big network. Therefore another approach based on the coordinated beamforming/scheduling has become popular recently [13], [14], [15].

The design objective that is considered in this thesis work is coordinated multi-cell minimum power beamforming. This approach satisfies some target SINR (signal to interference-noise ratio) for all users while minimizing the transmit power, which not only fulfills the quality of service for all users, irrespective of their distances, but also minimizes the interference level in general. Authors in [16] solve this problem for a single cell case using the duality in convex optimization theory which is shown to be linked to the concept of uplink-downlink duality. Then work in [17] extends the results to a multicell case. The other solution, as proposed by [18] and [19], formulates the problem as a second order cone which can be solved using the convex optimization tools.

The main target here is studying these solutions in the large dimensions regime. Authors in [20] use the work in [17] as the base for developing a large dimension approximation for the solution based on the uplink-downlink duality. Authors in [20] proves that these approximations simplify the algorithm and reduce the required inter base station exchange rate. However, the target SINR (signal to interference noise ratio) cannot be guaranteed and the resulting SINR might be less or more than the target SINR. In this thesis work, the second solution based on the SOCP is considered. The behavior of this algorithm is studied when dimensions grow large. Then possible simplifications are investigated in the large dimensions region. These studies have not been carried out before for the SOCP algorithm.

The results show that the performance gap with respect to ZF (zero forcing) and MF remains significant for a correlated antenna array, when the number of antennas grows up to a realistic limit, which justify the effort for characterizing the SOCP algorithm in

the large dimension regime. In addition, inter-cell interference term (that couples the sub-problems of each base station) is approximated using the random matrix theory tools. These approximations make it possible to predict the coupling term based on the statistics of the channel. It is shown that the optimal ICI for a system with large dimensions just depends on the channel statistics, thus the required exchange rate is inherently smaller when dimensions are large. Moreover, the predictable behavior of the optimal inter-cell interference term suggests a procedure for decoupling the SOCP subproblems. The decoupled subproblems can be solved independently while the user's positions are fixed.

The thesis is organized as follows: Chapter 2 is dedicated to massive MIMO, in which the results from literature are reviewed and the effects of imperfections such as: imperfect CSI and pilot contamination are studied. Random matrix theory is introduced in the same chapter, but the related lemmas and theories are presented in the appendix. At the end of this chapter, an overview about the antenna and propagation aspects clarifies the limits imposed on the performance of massive MIMO in a practical scenario. Chapter 3 deals with coordinated multi-cell minimum power beamforming. In this chapter, the solutions for the minimum power beamforming problem are investigated and their large dimension approximations are derived. The results of the simulations are presented in Chapter 4. The performance of the SOCP, MF and ZF algorithms are compared under two different user allocation strategy and system models. In addition, the performance of SOCP algorithm based on the instantaneous and average inter-cell interference is compared, which gives an idea about the validity of the large dimension approximations developed in Chapter 3.

2. MASSIVE MIMO

As discussed in the introduction, there are some interesting theoretical observations in the large antenna domain, which are subject to some practical considerations. In order to clarify these issues, the idea of massive MIMO from theoretical and practical perspectives are examined in this chapter. At first, the idea is presented using a simple model, then limitations and effects of imperfections are reviewed. Different beamforming and detection methods are studied and finally a short review over antenna and propagation aspects are presented.

2.1. Random matrix theory

Central limit theorem and law of large numbers are well known in the probability theory which characterize the mean of sufficiently large number of iterates of independent random variables and the mean of an experiment with a large number of trails, respectively. There are similar results about the large dimension behavior of matrix valued random variables. The mathematicians who were working on random matrices, observed that growing matrix dimensions resulted some eigenvalues with a distribution that converged weakly and almost surely to some deterministic distribution [6]. These predictable behaviors are very useful when dealing with a large dimensions system. Random matrix theory is the key tools for deriving and explaining the behaviors of massive MIMO. In appendix A a review of random matrix theory and some useful lemmas and theories are provided that are widely used throughout the thesis. The next section presents a very simple case, in which the law of large number describes the role of matched filter for detecting the user's data in an ideal scenario.

2.2. Massive MIMO in simple terms

It is known that the performance gains of a MIMO system increase with the number of antennas. On the other hand, some processing simplification results when the dimensions of the system grow large, which is due to the averaging properties of large dimension matrices. In order to make this clear, a simple model that relies on the matched filter for the detection purpose is considered which clarifies the idea of massive MIMO using some simple manipulations.

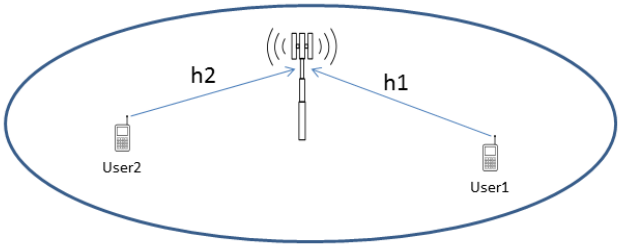

Figure 1: A simple model.

Figure 1 depicts a base station (BS) serving two single antenna users. The channel from each user is presented by $\mathbf{h}_i \in \mathbb{C}^{N_\mathrm{a}\times 1}$, where, N_a is the number of antennas at the BS. The entries of $\mathbf{h}_i$ are Gaussian distributed with zero mean and unit variance. It is assumed that the channels are known at the BS. The received signal at the BS is,

$$\mathbf{y} = \mathbf{h}_1 x_1 + \mathbf{h}_2 x_2 + \mathbf{w} \tag{1}$$

where,$\mathbf{n}$ is the noise vector, $\mathbf{n} \sim \mathbb{CN}(0, I)$. The BS applies a simple matched filter in order to detect the transmitted symbol of user 1. The matched filter for user 1 is given by $\frac{1}{|\mathbf{h}_1|}\mathbf{h}_1^H$. Then, the detection vector can be multiplied by $\frac{|\mathbf{h}_1|}{N_\mathrm{a}}$ without affecting its performance which gives,

$$\frac{1}{N_\mathrm{a}}\mathbf{h}_1^H\mathbf{y} = \overbrace{x_1\frac{1}{N_\mathrm{a}}\sum_{k=1}^{N_\mathrm{a}}(|h_{1,k}|^2)}^{\text{Desired}} + \overbrace{x_2\frac{1}{N_\mathrm{a}}\sum_{k=1}^{N_\mathrm{a}}(h_{1,k}^* h_{2,k})}^{\text{Interference}} + \overbrace{\frac{1}{N_\mathrm{a}}\sum_{k=1}^{N_\mathrm{a}}(h_{1,k}^* w_k)}^{\text{noise}} \tag{2}$$

Equation (2) shows the interference and noise parts which are undesired for the detection of user one's symbol. If $N_\mathrm{a} \to \infty$, according to the law of large number, the interference and noise terms go to $E[h_{1,k}^* h_{2,k}]$, $E[h_{1,k}^* w_k]$, respectively . These expectations are equal to zero because the elements inside the expectations are uncorrelated. Thus, the interference and noise terms disappear from the detected signal,

$$\frac{1}{N_\mathrm{a}}\mathbf{h}_1^H\mathbf{y} = x_1\frac{1}{N_\mathrm{a}}\sum_{k=1}^{N_\mathrm{a}}(|h_{1,k}|^2) \to x_1 E[|h_{1,k}|^2] = x_1 \tag{3}$$

This simple example shows the processing simplification resulted from increasing the dimension of the system. It is interesting that the effects of all uncorrelated parts disappear. Therefore under ideal assumptions a simple matched filter can be used for detection of user's data in uplink channel.

Using the same idea, downlink beamforming based on MF can be explained. However, it is possible to look at MF beamforming from a different view. In a LOS (line of sight) scenario, an antenna array can direct the beam towards a user in a specific direction by shifting the phase. When there is a non-LOS environment, directing of beam towards a direction does not have a clear meaning. In this case, one might consider focusing of energy to a geographical point in which components from different paths sum up constructively [4]. To make it clear, consider an antenna array with N_a antenna elements, covering an area. Also, assume that each antenna element corresponds to a path towards the users. Now, when the MF beamforming is used for a specific user, located in a geographical point, all N_a paths add up constructively at that point, which results in a good SNR (signal-to-noise ratio) for that specific user. However, other geographical points receive lower power, because the probability of constructive addition of all the paths in another point is quite small. Assuming fixed transmit power, it can be seen that increasing the number of antenna elements, decreases the power per antenna element, but increment the number of paths. Thus, the probability of constructive addition of all these low power paths become smaller, which is equivalent to a lower interference level. Thus, a base station with a large array can use simple MF beamforming without causing interference to other users, like the uplink detection in

(3). Nevertheless, it is important to note that these results are valid under some ideal assumptions with a large enough antenna array.

In this section, a simplified ideal scenario has been presented and it has been seen that the processing becomes simple when the antenna array grows large, in a way that MF becomes asymptotically optimal. In following sections more practical cases are considered and some other detection and beamforming methods are investigated.

2.3. Channel estimation and pilot contamination

2.3.1. Channel estimation using TDD or FDD

Base station (BS) needs channel knowledge for beamforming and coherent detection. The channel might be measured by users or BS, i.e the channel learning can be done using FDD or TDD.

In FDD, channel is estimated by users, using a downlink training sent by BS. Then, the estimated channel is fed back to the BS. Thus, the pilot overhead is proportional to the number of antennas which makes FDD impractical when the antenna array at the BS grows large. However, under some assumptions, it is possible to use FDD for learning the channels in the large antenna array case [21].

TDD is based on reciprocity of downlink and uplink channels (downlink channel is transpose of uplink channel). Therefore, BS can learn the uplink channel and use it for beamforming or detection purposes. Even though the reciprocity is applicable for the physical channel, it is not valid for a transceiver RF chain without calibration. Work in [22] has studied different calibration methods for the RF chains. In TDD mode, the number of antennas at BS side does not affect the pilot overhead, while the number of users defines this parameter because some orthogonal pilots are required for learning user's channels. Therefore, the number of users is restricted by the number of available orthogonal pilots. For example, assume that the coherence bandwidth of a channel covers N_{s} sub-carriers and the total number of users is equal to N_{u}. Then, N_{ts} time slots are required for estimation of the uplink channel, where $N_{\mathrm{ts}} = \frac{N_{\mathrm{u}}}{N_{\mathrm{s}}}$. In addition, the channel must be fixed during these time slots, i.e, duration of the training multiplied by the number of time slots must be smaller than the coherence time. The data transmission period is not considered in this calculations for simplicity, which is not a reasonable assumption. However, it gives an idea about the limitation imposed by the number of available orthogonal pilots over the number of users which can be served within the same frequency and time resources.

As described above, the TDD scheme seems a suitable choice when there is a large antenna array at the BS side. Therefore, throughout the rest of this thesis, TDD will be assumed as the method for channel estimation.

2.3.2. Channel estimation error, pilot contamination and other imperfections

In order to study the effects of imperfect channel estimation and pilot contamination, the same procedure as [23] is followed. Consider a multi cell system with N_{c} cells and some single antenna users in each cell that are served by a BS with N_{a} antennas. Here,

for simplicity, N_c is assumed to be equal to 2 and one user is considered in each cell. This scenario is illustrated in Figure 2. In the figure, $\mathbf{h}_{b,k}$ is the channel from the b^{th} BS to the k^{th} user. It is assumed that user 1 and user 2 are in cell 1 and cell 2, respectively. The channels are assumed to undergo flat fading with the same frequency band reused on all the cells.

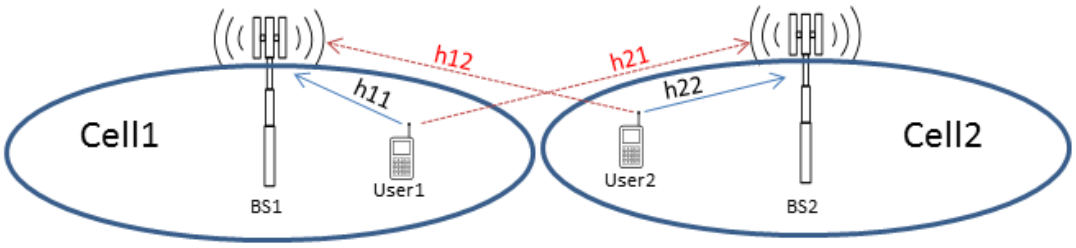

Figure 2: Two cells with pilot contamination from the neighboring cells.

During the uplink training, the users in each cell transmit their pilots. The pilots for the users in each cell are orthogonal but the same set of pilots is reused in the neighboring cell. Figure 2 shows the two cell case with users 1 and user 2, who use the same pilot sequence. BS 1 correlates the received signal with the pilot sequence assigned to user one for estimating $\mathbf{h}_{11}$ and get [23],

$$\mathbf{y} = \mathbf{h}_{11} + \mathbf{h}_{12} + \frac{1}{\sqrt{\rho_{\text{t}}}}\mathbf{n} \tag{4}$$

Where ρ_{t} is the effective training SNR, which is determined by the pilot power and the length of the pilot sequence [23]. User 1 and user 2 use the same pilot sequence, therefore, the other user's channel also appears in the detected signal when the base station correlates the received signal with the pilot sequence of user 1.

Based on the detected signal $\mathbf{y}$, BS 1 calculates the MMSE (minimum mean square error) estimate of $\mathbf{h}_{11}$ [24],

$$\breve{\mathbf{h}}_{11} = \mathbf{K}_{11}(\mathbf{K}_{12} + \mathbf{K}_{11} + \frac{1}{\rho_{\text{t}}}\mathbf{I}_{\text{N}_\text{a}})^{-1}(\mathbf{y}) \tag{5}$$

$$\mathbf{K}_{ij} = E[\mathbf{h}_{ij}\mathbf{h}_{ij}^{H}] \tag{6}$$

$\breve{\mathbf{h}}_{11}$ in (5) is the MMSE estimate of $\mathbf{h}_{11}$, when both users use the same pilot. It can be seen that the estimate of $\mathbf{h}_{11}$ is correlated with $\mathbf{h}_{12}$, i.e. the reused pilots from the neighboring cell corrupt the channel estimate of the local users. This phenomenon is known as pilot contamination.

Moreover, the estimate of the channel is not perfect and there is an estimation error. MMSE is based on principle of orthogonality, according to which it is possible to present $\mathbf{h}_{11} = \breve{\mathbf{h}}_{11} + \tilde{\mathbf{h}}_{11}$,where $\breve{\mathbf{h}}_{11} \sim \mathbb{CN}(0, \boldsymbol{\Theta}_{\mathbf{11}})$ is the MMSE estimate of $\mathbf{h}_{11}$ and $\tilde{\mathbf{h}}_{11} \sim \mathbb{CN}(0, \mathbf{K}_{11} - \boldsymbol{\Theta}_{11})$ is the estimation error which is uncorrelated with $\breve{\mathbf{h}}_{11}$. The covariance matrix of the estimate is defined as follows,

$$\boldsymbol{\Theta}_{\mathbf{11}} = \mathbf{K}_{11}(\mathbf{K}_{11} + \mathbf{K}_{12} + \frac{1}{\rho_{\text{t}}}\mathbf{I}_{\text{N}_\text{a}})^{-1}\mathbf{K}_{11} \tag{7}$$

Now, assume that the users transmit their data symbols through the uplink channel and the base station uses the above MMSE estimate for detection of the user one's data. The received signal at the base station can be presented as follows,

$$\mathbf{y}_{\text{data}} = (\breve{\mathbf{h}}_{11} + \tilde{\mathbf{h}}_{11})x_1 + \mathbf{h}_{12}x_2 + \frac{1}{\sqrt{\rho}}\mathbf{n} \tag{8}$$

Where, ρ is the SNR used for data transmission. From this equation, it is easy to derive the SINR for user 1, when the BS uses the matched filter as the detection vector,

$$\gamma_1 = \frac{||\breve{\mathbf{h}}_{11}||^4}{\breve{\mathbf{h}}_{11}^{\ H}(\mathbf{h}_{12}\mathbf{h}_{12}^H + \tilde{\mathbf{h}}_{11}\tilde{\mathbf{h}}_{11}^{\ H} + \frac{1}{\rho}\mathbf{I}_{\text{N}_\text{a}})\breve{\mathbf{h}}_{11}} \tag{9}$$

The effects of noise, pilot contamination, imperfect CSI and interference is already visible in the dominator of the above equation. However, a large dimension approximation for the SINR term provides a better view about the behavior of these parameters. This approximation is independent of the instantaneous channels, thus, the result can be expressed as a function of the statistics of the channels. Authors in [23] show that the large dimension approximation for the SINR based on the MF detection contains the effect of all of these undesired parameters, i.e. the SINR term for the MF detection can be written as,

$$\gamma_1 = \frac{(\frac{1}{N_\text{a}} tr\mathbf{\Theta_{11}})^2}{\text{Interference + Imperfect CSI + Noise + Pilot contamination}} \tag{10}$$

The details of these approximations are ignored because it is not in the scope of the study here. The interested reader can refer to section III of the work in [23] for further details. Nevertheless, the authors in [23] show that the approximation for a simplified system model gives a straightforward expression for the SINR, which explains the effects of these imperfections in a simple term. In this model, the channels are assumed to have following structure (for more information refer to the work in [23], section IV),

$$\mathbf{H}_{j,\mathcal{U}_j} = \sqrt{\frac{N_\text{a}}{N_\text{d}}}\mathbf{A}\mathbf{V}_{jj} \tag{11}$$

$$\mathbf{H}_{j,\mathcal{U}_l} = \sqrt{\alpha\frac{N_\text{a}}{N_\text{d}}}\mathbf{A}\mathbf{V}_{jl}\,, l \neq j \tag{12}$$

Where, $\mathbf{H}_{j,\mathcal{U}_l}$ is a matrix with the columns equal to the channel vectors from the j^{th} BS to all the users in the l^{th} cell. $\mathbf{A} \in \mathbb{C}^{N_\text{a} \times N_\text{d}}$ is a matrix with the column vectors taken from a $N_\text{a} \times N_\text{a}$ unitary matrix. $\mathbf{V}_{lj} \in \mathbb{C}^{N_\text{d} \times N_\text{u}}$ are standard complex Gaussian matrices. $\alpha \in (0, 1]$ is the intercell interference factor that indicates the strength of the interference from the neighboring cells. In this system model, N_d is the number of d.o.f provided by the channels, which is smaller but not necessarily equal to N_a. A detailed discussion about the relation between N_d and N_a is presented in section 2.4. Authors in [23] show that the large dimension approximation of the SINR based on MF detection for this simplified model can be expressed as,

$$\gamma_1 = \frac{1}{\underbrace{\frac{\widetilde{N_{\mathrm{c}}}}{\rho N_{\mathrm{a}}}}_{\text{Noise}} + \underbrace{\frac{1}{\rho_{\mathrm{t}}}(\frac{\frac{N_{\mathrm{d}}}{N_{\mathrm{a}}}}{\rho N_{\mathrm{a}}} + \frac{N_{\mathrm{u}}}{N_{\mathrm{a}}}\widetilde{N_{\mathrm{c}}})}_{\text{Imperfect CSI}} + \underbrace{\frac{N_u}{N_{\mathrm{d}}}\widetilde{N_{\mathrm{c}}}^2}_{\text{Interference}} + \underbrace{\alpha(\widetilde{N_{\mathrm{c}}} - 1)}_{\text{Pilot contamination}}} \tag{13}$$

$$\widetilde{N_{\mathrm{c}}} = 1 + \alpha(N_{\mathrm{c}} - 1) \tag{14}$$

In the next section, it is seen that the number of degrees of freedom (d.o.f) is not only related to the number of antennas, but also it depends on the scattering environment, which justifies the existence of N_{d} in this formula. From (13), the following results can be inferred [23] [25]:

- Interference vanishing rate is related to $N_{\mathrm{d}}/N_{\mathrm{u}}$, not $N_{\mathrm{a}}/N_{\mathrm{u}}$. Therefore, interference diminishes by increasing the number of antennas provided that the environment offers additional degrees of freedom. However, more antennas result in a bigger SNR even with a saturated degrees of freedom.

- Assuming the noise to be the only limiting factor for SINR, it can be seen from (13) that the SNR is a linear function of ρ. Thus, it is possible to get a higher SNR by increasing the number of antennas, without incrementing the transmit power.

- Assuming $\rho = \rho_{\mathrm{t}} \sim 1/N_{\mathrm{a}}^{-c}$, i.e allowing the transmit and pilot power to decrease proportional to the inverse of N_{a}, from (13), one can see that for $c > 0.5$ the effect of imperfect CSI does not disappear with a large N_{a}. Therefore, for a fixed SINR constraint, the transmit power can be decreased proportional to $\frac{1}{\sqrt{N_{\mathrm{a}}}}$, when CSI is imperfect, while with perfect CSI, the rate of decrease of power is proportional to $\frac{1}{N_{\mathrm{a}}}$.

- Finally when the number of d.o.f grows with the number of antennas towards infinity, effects of noise, interference and imperfect CSI disappear, but pilot contamination remains the only limiting factor.

Now, using the SINR in (13), it is possible to present the ultimate achievable rate as follows [23],

$$R_{\mathrm{N_d,N_a}\to\infty} = log_2(1 + \frac{1}{\alpha(\widetilde{N_{\mathrm{c}}} - 1)}) \tag{15}$$

It is interesting that all the limiting factors other than pilot contamination have disappeared from the ultimate rate formulation. With $\alpha = 0$, there is no pilot contamination. In this case the SINR can be increased without bound by incrementing N_{d} and N_{a}. Even though the pilot contamination remains as the limiting factor in the large antenna array regime, there are different mitigation methods. For example works in [26], [27], [28], [29], [30] present different methods for overcoming this problem.

Until now interference, noise, pilot contamination and imperfect CSI are studied as some restricting factors that appear in a common cellular networks. However, there are some other bounds in practice that must be treated carefully. For example, authors in [31] consider the effects of hardware imperfection. Generally hardware imperfection

causes the emitted signal to be different from the desired one. Also it causes distortion in the received signal. Hardware imperfection of BS and user equipment cause errors in channel estimate [31] . It is interesting that this error does not vanish by increasing the pilot power, which results in an error floor for the channel estimate as a function of the average SNR [31] . Authors in [31] show that hardware imperfection is a limiting factor at the large antenna array domain which restricts the capacity when the number of antennas grows large.

In this section the idea of Massive MIMO and the related restrictions have been presented using an uplink channel with a MF detection. However, the optimality of MF has not been discussed yet. Thus, Section 2.5 is dedicated to other detection/beamforming methods. The comparison carried out between MF and other algorithms shows that MF is just asymptotically optimal for two cases, one when SNR$\rightarrow 0$ and the other when $N_{\mathrm{a}} \rightarrow \infty$. Prior to that, the issues related to antenna and propagation are considered which clarify the limits imposed in practice.

2.4. Antenna and propagation

Throughout the last sections, a specific channel has been considered as the desired one for a massive MIMO system. Considering the random matrix theory (RMT) results as the benchmark, one might describe a channel with i.i.d elements as the desired channel. However, the channel realizations that appear in practice are not always i.i.d, for example correlation among the elements of an antenna array causes correlations among the channel entries. In this section the practical restrictions and considerations are presented that helps on understanding the limitations that must be taken into account when analyzing the results from the theory.

The first restriction on a large array is implementation space. Limited implementation space and non-ideal radiation pattern, result in correlation among antenna elements [4]. From the previous section, it is known that vanishing rate of interference depends on the number of d.o.f. On the other hand, a correlated antenna array generally provides a number of d.o.f less than the number of antenna elements. Thus, correlation among antenna elements seems as an undesired parameter. Nevertheless, work in [21] shows that under some specific assumption about the correlation matrices, inter antennas correlation can increases the orthogonality of the channels. However, without any special assumption, correlation should be considered as an undesired parameter. For example, the simulations in Chapter 4 shows that increasing the correlation among the antenna elements degrades the performance of different detection and beamforming methods.

Another parameter to be considered is mutual coupling among antenna elements. It is desired to pack the antenna elements in a small area. However, the small distances among the antennas result in mutual coupling among the elements. Mitigating the effects of mutual coupling has been studied in different references. Nevertheless applying these methods result in a reduction of bandwidth and introduction of ohmic losses (due to matching circuits), which degrade the system performance [32] [4]. Authors in [4] have studied the effects of correlation and coupling via simulation. This simulation shows that the performance of a system with correlation is worse than the i.i.d case. However, coupling can cause smaller correlation for some special antenna

element spacing (in a ULA antenna array), which makes the performance better compared to the correlation only case. However, coupling generally degrades the system performance [4].

Another limitation is imposed by the propagation medium. In order to get a channel matrix with i.i.d elements, a rich and distinct scattering medium is required. As reported in [4] [33], the scatterers appear in groups (clusters) which result in a correlated multipath components. Also the clusters that are common among users result in inter user correlation. It means that the number of d.o.f offered by the channel depends also on the propagation medium. One might conclude that a LOS channel is not favorable but it should be noted that the large array has a good spatial resolution which results in the distinction of the users with adequate angular separation [3]. Thus, even a LOS channel can be favorable when a suitable user scheduling algorithm is applied.

It can be concluded that coupling and correlation can be useful under some specific conditions. However, without any specific assumption, correlation and coupling degrade the performance of massive MIMO. Also, the number of d.o.f not only depends on the number of antenna elements but also on the propagation medium and some other parameters.

2.5. Detection and beamforming methods

A comparison among different beamforming/detection methods is carried out in Chapter 4 by simulation. However, in this section a literature review is presented, in which large dimension approximations are used for comparing different algorithms.

Until now just matched filter (MF) is considered as a beamforming/detection method, Nevertheless optimality of MF is arguable. Authors in [23] have studied different linear beamforming/detection methods such as: MF, MMSE and regularized zero forcing (RZF). Their study is based on the large dimension approximation for the SINR formula. Nevertheless, their simulation results show that approximations for large dimensions are almost valid for finite dimensions. Thus, the approximated SINR formulas can be applied for comparing different methods in practice. From their results it can be inferred that MMSE/RZF achieves the same performance as MF detection/beamforming with a smaller number of d.o.f. For example, consider the simplified system model presented in Section 2.3.2 (with $\alpha = 0.3$), it can be shown that for $\rho N_{\mathrm{a}} = 25dB$ (effective SNR), MMSE/RZF with 100 d.o.f achieve 95% of $R_{\mathrm{N_d},\mathrm{N_a}\to\infty}$ (defined by (15)) , while the MF detection/beamforming needs 50 more d.o.f in order to achieve the same performance [23].

Another analysis have been carried out by authors in [4] for an asymptotic regime where the number of users and antennas grows large with a fixed ratio, i.e $N_{\mathrm{a}}, N_{\mathrm{u}} \to \infty$, while $N_{\mathrm{a}}/N_{\mathrm{u}} = c$. In this model, the received signal for user k is,

$$\mathbf{y}[k] = \mathbf{h}_k^H \mathbf{x}_k + \sum_i \mathbf{h}_i^H \mathbf{x}_i + \mathbf{n}_k \tag{16}$$

Where, the entries of $\mathbf{h} \sim \mathbb{CN}(0,1)$ are assumed i.i.d. The data symbols (d_k) are precoded by a beamforming vector $\mathbf{w}_k$ such that the elements of $\mathbf{x}_k = \mathbf{w}_k d_k$ has an average power equal to ρ/N_{a}. Also it is assumed that $E[d_k^H d_k] = \frac{\rho}{N_{\mathrm{u}}}$

Work in [4] uses interference free (IF) system as a benchmark for comparing MF beamforming and ZF beamforming techniques. In an interference free system, the signal intended for each user, can be delivered to the user without causing interference to others. In this case it is easy to see that the SINR converges to ρc when $N_{\mathrm{a}} \to \infty$.

With some simple mathematical calculation, authors in [4] show that under perfect CSI, the SINR of ZF goes to $\rho(c-1)$ i.e. ZF achieves the same performance as an IF system with $N_{\mathrm{a}} - N_{\mathrm{u}}$ antennas. On the other hand, the MF beamforming gets a SINR equal to $\frac{\rho c}{\rho+1}$. One can observe that the SINR of MF beamforming can be scaled up by scaling the c value, but for $\rho \to \infty$, the SINR has finite ceiling equal to c, i.e the SINR of the MF beamforming shows an error floor when plotted as a function of SNR.

Then authors in [4] consider the same scenario with an imperfect channel estimate. Assuming a MMSE estimate, it is possible to present the estimate of channel as follows,

$$\mathbf{H} = \xi\mathbf{H} + \sqrt{1-\xi^2}\mathbf{E} \tag{17}$$

$$\mathbf{H} = [\mathbf{h}_1, ..., \mathbf{h}_{N_{\mathrm{u}}}] \tag{18}$$

Where $0 < \xi \leq 1$ shows the accuracy of the channel. The error of the channel estimate is represented by $\mathbf{E}$ which is a matrix with i.i.d $\mathbb{CN}(0,1)$ distributed elements. Under imperfect channel estimate assumption, it can be shown that the SINR of ZF converges to $\frac{\xi^2\rho(\alpha-1)}{(1-\xi^2)\rho+1}$, while the SINR of MF beamforming goes to $\frac{\xi^2\rho\alpha}{\rho+1}$ [4]. It is clear from this approximations that the imperfect channel estimate restricts the achievable SINR for both of the ZF and MF beamforming when c value is fixed. However, the SINR value can be incremented as much as desired by increasing the $N_{\mathrm{a}}/N_{\mathrm{u}} = c$ ratio.

In addition to the simple methods discussed above, there are more efficient algorithms that are already studied for cellular MIMO networks. These methods become interesting when the limits imposed in practice are taken into account. When such restrictions are applied, the gap between optimal and sub-optimal methods get larger and application of more efficient methods becomes attractive. One of such a approaches is CoMP (coordinated multi-point) which is already considered in 3GPP standard. CoMP utilizes cooperation between nodes for delivering services to users which result in reduction of interference level and transmit power [9]. The CoMP method that is considered in this thesis work is coordinated multi-cell minimum power beamforming. This approach allows sharing control information between nodes for making a joint decision about the beamforming vectors. This beamforming problem is introduced in Chapter 3 and possible solutions are investigated. Then large dimension approximations for these solutions are developed using random matrix theory tools. Finally in Chapter 4 performance of this algorithm is compared to other sub-optimal methods using simulation.

2.6. Summary and discussion

In this chapter the motivation for increasing the number of antenna elements in a MIMO system has been presented and the theory behind massive MIMO has been

investigated. It was seen that increasing the number of antennas at BS, not only increments the capacity but also simplifies the processing. This is due to the fact that random phenomena become deterministic and noise and fading disappear. Also different limiting factors and practical considerations have been studied and a brief review over the antenna and propagation aspects has been pursued.

Finally, it worth to mention that in practice, Massive MIMO works below the ultimate ideal performance. For example work in [23] shows that for the simplified system model in section 2.3.2, the MF beamforming needs 150 d.o.f per user, for achieving 95 percent of the ideal performance (for the effective SNR equal to 25dB).

3. COORDINATED MULTI-CELL MINIMUM POWER BEAMFORMING

Large antenna array in a MIMO system simplifies the processing (due to the averaging nature of a large array), in a way that even matched filter can be used asymptotically in an ideal i.i.d channel for detection and beamforming. Nevertheless, in Chapter 2, it has been seen that the other methods such as MMSE/RZF, can achieve the same performance as MF detection/beamforming with a smaller number of d.o.f. On the other hand, in practice the number of d.o.f is limited by some restricting factors. Therefore, it is more reasonable to take into account the application of a more optimal methods which utilizes the available number of d.o.f efficiently.

In this thesis, coordinated multi-cell minimum power beamforming is considered as such optimal approach. The behaviors of this algorithm in large antenna array domain are characterized and possible simplifications resulting from the large dimension approximations are investigated. The performance of several methods are compared to the optimal schemes for a MIMO system with a large antenna array in different deployment scenarios. This chapter is dedicated to the introduction of the minimum power beamforming problem and possible solutions. Then in the next chapter further analysis will be carried out on a candidate solution.

3.1. System model

A cellular system is considered which consists of N_{B} BSs, each BS has N_{a} transmit antennas. Each user has a single receive antenna. Users allocated to the b^{th} base station are in set $\mathcal{U}_b$. A user can be served by multiple synchronized BSs and the set of BSs that serve user k is $\mathcal{B}_k$. Sets of all users and all BSs are presented by $\mathcal{B}$ and $\mathcal{U}$ respectively. The signal for user k consists of the desired signal, the intracell and the intercell interference (as depicted by Figure 4) which can be presented as follows:

$$\mathbf{y}[k] = \sum_{b\in\mathcal{B}_k} \mathbf{h}_{b,k}^H \mathbf{x}_{b,k} + \sum_{b\in\mathcal{B}_k} \mathbf{h}_{b,k}^H \sum_{l\in\mathcal{U}_b\neq k} \mathbf{x}_{b,l} + \sum_{b\in\mathcal{B}\neq\mathcal{B}_k} \mathbf{h}_{b,k}^H \sum_{l\in\mathcal{U}_b} \mathbf{x}_{b,l} + \mathbf{n}_k \qquad (19)$$

In this equation $\mathbf{n}_k \sim \mathbb{CN}(0, N_0)$ is the noise with power density N_0. $\mathbf{h}_{b,k} \in \mathbb{C}^{N_{\mathrm{a}}}$ represents the channel from the b^{th} BS to k$^{\text{th}}$ user. The channels are assumed Rayleigh and the path-losses are included in the channel vectors. $\mathbf{x}_{b,k} = \mathbf{w}_{b,k} d_k$ is the transmitted vector from the b^{th} BS to k$^{\text{th}}$ user, in which, d_k is the normalized complex data symbol ($E[|d_k|^2] = 1$) and $\mathbf{w}_{b,k} \in \mathbb{C}^{N_{\mathrm{a}}}$ is the beamforming vector from the b^{th} BS to k$^{\text{th}}$ user.

Now the SINR for the k^{th} user can be expressed as:

$$SINR_k = \frac{|\sum_{b\in\mathcal{B}_k} \mathbf{h}_{b,k}^H \mathbf{w}_{b,k}|^2}{N_0 + \sum_{l\in\mathcal{U}\neq k} |\sum_{b\in\mathcal{B}_l} \mathbf{h}_{b,k}^H \mathbf{w}_{b,l}|^2} \qquad (20)$$

Throughout this chapter a narrow band flat fading scenario is assumed, in which, the set of active users is served over the same frequency band.

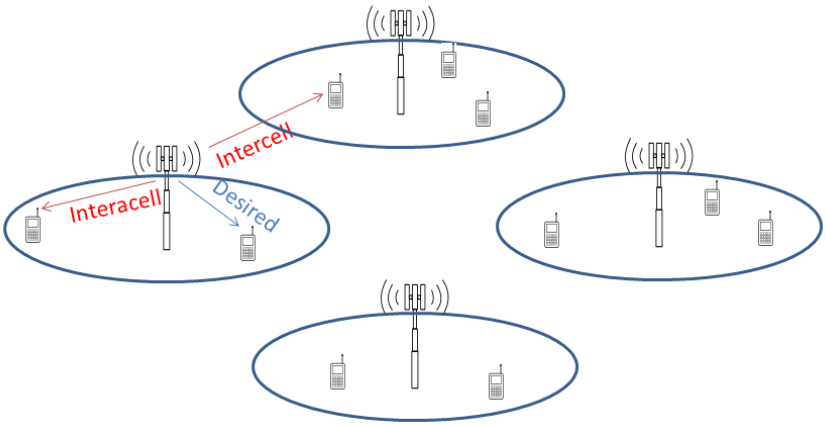

Figure 3: A multicell system with intercell and intracell interference

3.2. Optimization problem for minimum power beamforming

The optimization objective in the minimum power beamforming is minimization of the sum power such that some specific SINR constraints are satisfied. The optimization problem can be solved in various manners. This algorithm is suitable for practical scenarios, because with some strict quality of service (QOS) constraints, the fairness is guaranteed for all users, independent of the distances. Moreover, with the minimum power transmission, less interference is emitted in general. The optimization problem is,

$$\begin{aligned} \underset{\mathbf{w}_{b,k}}{\text{minimize}} \quad & \sum_{b\in\mathcal{B}}\sum_{k\in\mathcal{U}_b} |\mathbf{w}_{b,k}|^2 \\ \text{subject to} \quad & \frac{|\mathbf{h}_{b_k,k}^H \mathbf{w}_{b_k,k}|^2}{N_0 + \sum_{l\in\mathcal{U}_{b_k}\setminus k} |\mathbf{h}_{b_k,k}^H \mathbf{w}_{b_k,l}|^2 + \sum_{b\in\overline{\mathcal{B}_k}}\sum_{l\in\mathcal{U}_b} |\mathbf{h}_{b,k}^H \mathbf{w}_{b,l}|^2} \forall k \in \mathcal{U} \end{aligned} \tag{21}$$

where, the target SINR for user k is denoted by γ_k and $\overline{\mathcal{B}_k}$ is the set complement to $\mathcal{B}_k$. The presented system model and the optimization problem are for a general case where several base stations serve a user jointly, however, in the next sections it is assumed that each user is served by a single base station (unless explicitly mentioned) which makes the problem and formulations simpler. In this case the optimization problem becomes,

$$\begin{aligned} \underset{\mathbf{w}_{b,k},\epsilon_{b,k}}{\text{minimize}} \quad & \sum_{b\in\mathcal{B}}\sum_{k\in\mathcal{U}_b} |\mathbf{w}_{b,k}|^2 \\ \text{subject to} \quad & \frac{|\mathbf{h}_{b_k,k}^H \mathbf{w}_{b_k,k}|^2}{N_0 + \sum_{l\in\mathcal{U}_{b_k}\setminus k} |\mathbf{h}_{b_k,k}^H \mathbf{w}_{b_k,l}|^2 + \sum_{b\in\overline{\mathcal{B}_k}} (\epsilon_{b,k})^2} \geq \gamma_k \ \forall k \in \mathcal{U}_b, \forall b, \\ & \sum_{l\in\mathcal{U}_b} |\mathbf{h}_{b,k}^H \mathbf{w}_{b,l}|^2 \leq (\epsilon_{b,k})^2, \forall k \notin \mathcal{U}_b, \forall b, \end{aligned} \tag{22}$$

where, b_k denotes the BS that serves user k and intercell interference from b^{th} base station to user k is denoted by $\epsilon^2_{b,k}$ which is relaxed with an inequity constraint. However, it hold with equality at the optimal solution and the optimal values for (22) are equivalent to (21) with $\mathcal{B}_k = b_k$. This formulation indicate that the intercell interference is the parameter that couples the beamforming subproblems at base stations.

The next sections study two possible solutions for this problem. The first one solves the problem by formulating the constraint as a second order cone. This solution is the focus of the study in the next chapter. The other solution is based on the downlink-uplink duality which is introduced in Section 3.3.2.

3.3. Possible solutions for minimum power beamforming

3.3.1. Beamforming via SOCP

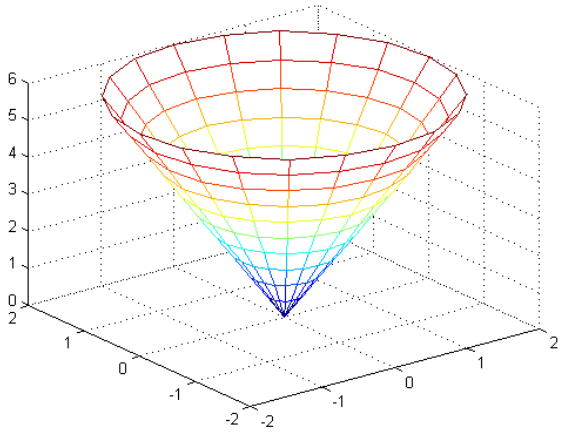

Figure 4: Second order cone in $\mathbb{R}^3$, $\sqrt{x_1^2 + x_2^2} \leq r$

The optimization problem defined by (21) can be formulated as a second order cone problem (SOCP) and be solved in a centralized manner [19]. In order to formulate the problem as a SOCP, it is assumed that each user is served by a single BS which makes the problem simpler. Nevertheless, it can be shown that it is also true for the general case in (21).

The SINR constraints at the optimal point are satisfied with equality, therefore, the constraints can be presented as follows [18],

$$\frac{1}{\gamma_k}|\mathbf{h}^H_{b_k,k}\mathbf{w}_{b_k,k}|^2 = N_0 + \sum_{l\neq k}|\mathbf{h}^H_{b_l,k}\mathbf{w}_{b_l,l}| \tag{23}$$

Where, b_k indicates the BS that serves the k$^{\text{th}}$ user. Then, by adding $|\mathbf{h}^H_{b_k,k}\mathbf{w}_{b_k,k}|^2$ to both sides of the above equation,

$$(\frac{1}{\gamma_k} + 1)|\mathbf{h}^H_{b_k,k}\mathbf{w}_{b_k,k}|^2 = N_0 + \sum_{l}|\mathbf{h}^H_{b_l,k}\mathbf{w}_{b_l,l}| \tag{24}$$

Note that $|\mathbf{h}_{b_k,k}^H \mathbf{w}_{b_k,k}|^2$ can be replaced with $e^{-j\theta}(\mathbf{h}_{b_k,k}^H \mathbf{w}_{b_k,k})^2$, where θ cancel the phase of complex product. $e^{-j\theta}$ can be ignored without affecting the SINR, Therefore, by taking square root of both sides, the constraints becomes,

$$\sqrt{(\frac{1}{\gamma_k}+1)}(\mathbf{h}_{b_k,k}^H \mathbf{w}_{b_k,k}) = \sqrt{N_0 + \sum_l |\mathbf{h}_{b_l,k}^H \mathbf{w}_{b_l,l}|^2} \tag{25}$$

Now, (21) can be presented in epigraph form [34] as follows,

$$\begin{aligned} \underset{\mathbf{w}_{b,k}}{\text{minimize}} \;\; & P \\ \text{subject to} \;\; & \left| \begin{array}{c} \mathbf{W}^H \mathbf{h}_{b,k} \\ N_0 \end{array} \right| \leq \sqrt{(\frac{1}{\gamma_k}+1)}(\mathbf{h}_{b,k}^H \mathbf{w}_{b,k}), \;\; \forall k \in \mathcal{U}, \\ & |vec(\mathbf{W})| \leq P \end{aligned} \tag{26}$$

where, $\mathbf{W} = [\mathbf{w}_{1,\mathcal{U}_1(1)}, ..\mathbf{w}_{|\mathcal{B}|,\mathcal{U}_{|\mathcal{B}|}(\text{end})}]$ i.e. the vector that contains all the beamforming vectors.

Equation (26) presents the problem in the standard form of SOCP [34] which makes it possible to solve the downlink minimum power beamforming problem using the convex optimization tools efficiently. However, this centralized solution requires the channel knowledge of all $\mathbf{h}_{b,k}$ which is not a practical solution. Thus, in the next step a decentralized approach is proposed which solves the problem in a decentralized manner.

Authors in [19] propose a decentralized solution by using dual decomposition (there are also alternative solutions based on primal decomposition [35] and ADMM (alternating direction method of multipliers) [36]). Looking at (21), it can be seen that the primal problem is a combination of several subproblems (one subproblem per BS) which are coupled via the inter-cell interference terms. This coupling term can be presented as a coupling constraint (see (27)) [19]. When there is such a coupling constraint, one can decouple the primal problem into several subproblems using dual decomposition approach [34].

$$\begin{aligned} \underset{\mathbf{w}_{b,k},\epsilon_{b,k}}{\text{minimize}} \;\; & \sum_{b\in\mathcal{B}} \sum_{k\in\mathcal{U}_b} |\mathbf{w}_{b,k}|^2 \\ \text{subject to} \;\; & \frac{|\mathbf{h}_{b_k,k}^H \mathbf{w}_{b_k,k}|^2}{N_0 + \sum_{l\in\mathcal{U}_{b_k}\setminus k} |\mathbf{h}_{b_k,k}^H \mathbf{w}_{b_k,l}|^2 + \sum_{\hat{b}\in\overline{\mathcal{B}_k}} (\epsilon_{\hat{b},k}^{b_k})^2} \geq \gamma_k \;\; \forall k \in \mathcal{U}_b, \forall b, \\ & \sum_{l\in\mathcal{U}_b} |\mathbf{h}_{b,k}^H \mathbf{w}_{b,l}|^2 \leq (\epsilon_{b,k}^{b_k})^2, \forall k \notin \mathcal{U}_b, \forall b, \\ & (\epsilon_{b,k}^{b}) = (\epsilon_{b,k}^{b_k}), \forall k, b \in \overline{\mathcal{B}_k}, \end{aligned} \tag{27}$$

In (27), the b_k subscript indicates the base station that serves the k$^{\text{th}}$ user. The inter-cell interference from the b^{th} base station to the k$^{\text{th}}$ user is donated by $\epsilon_{b,k}^2$. The superscript of $\epsilon_{b,k}^b$ indicates the local copy of $\epsilon_{b,k}$ at the b^{th} base station and $\epsilon_{b,k}^b = \epsilon_{b,k}^{b_k}$ constraint enforces the local copies to be equal. $\overline{\mathcal{B}_k}$ means the set of base stations that does not serve the k^{th} user.

As suggested in [19], a standard dual decomposition approach is taken which relaxes the consistency constraint ($\epsilon_{b,k}^{b} = \epsilon_{b,k}^{b_k}$) by taking a partial lagrangian (for more information refer to work in [19], part B). It can be shown that the original problem can be transferred into the subproblems defined by (28), at each base station [19]. The consistency prices ($\mathbf{c}_b$) are set by a master problem which can be solved by an iterative sub-gradient method, as shown in (29).

$$\begin{aligned} \underset{\mathbf{w}_{b,k}}{\text{minimize}} \quad & \sum_{k\in\mathcal{U}_b} |\mathbf{w}_{b,k}|^2 + \mathbf{c}_b^T \boldsymbol{\epsilon}^b \\ \text{subject to} \quad & \frac{|\mathbf{h}_{b_k,k}^H \mathbf{w}_{b_k,k}|^2}{N_0 + \sum_{l\in\mathcal{U}_{b_k}\setminus k} |\mathbf{h}_{b_k,k}^H \mathbf{w}_{b_k,l}|^2 + \sum_{\hat{b}\in\overline{\mathcal{B}_k}} (\epsilon_{\hat{b},k}^{b_k})^2} \geq \gamma_k \ \forall k \in \mathcal{U}_b \\ & \sum_{l\in\mathcal{U}_b} |\mathbf{h}_{b,k}^H \mathbf{w}_{b,l}|^2 \leq (\epsilon_{b,k}^{b_k})^2, \forall k \notin \mathcal{U}_b \end{aligned} \tag{28}$$

In the above equation, $\boldsymbol{\epsilon}^b$ is a vector which contains $\boldsymbol{\epsilon_k}^b = [\epsilon_{\overline{\mathcal{B}_k}(1),k}^{b}, ..., \epsilon_{\overline{\mathcal{B}_k}(|\overline{\mathcal{B}_k}|),k}^{b}] \ \forall k \in \mathcal{U}_b$ and $\epsilon_{b,k}^{b} \ \forall k \notin \mathcal{U}_b$.

The master problem sets the consistency prices ($\mathbf{c}$) by using the sub-gradient update [19],

$$c_{b,k}(t) = c_{b,k}(t) + u(\epsilon_{b,k}^{b} - \epsilon_{b,k}^{b_k}) \ \forall b, k \tag{29}$$

In which, u defines the step size and t is the iteration index.

To sum up, the decentralized coordinated multicell beamforming algorithm as proposed by [19] is presented as follows,

1. Initialize the consistency prices to some initial values.
2. Solve (28) at each BS and exchange the resulted $\epsilon_{b,k}$ between the coupled base stations
3. Get the new consistency prices using (29).
4. Repeat the above steps till convergence.

According to this algorithm, $\epsilon_{b,k}^{b}$ and $\epsilon_{b,k}^{b_k}$ must be exchanged among the coupled base stations at each iteration. Authors in [19] show that the maximum amount of information exchange (without clustering) can be expressed as,

$$2 \times \sum_{b=1}^{N_\mathrm{B}-1} \sum_{i=b+1}^{N_\mathrm{B}} (|\mathcal{U}_b| + |\mathcal{U}_j|) \tag{30}$$

It is clear that the amount of exchanged data depends on the number of users and base stations, while it is independent of the number of antennas at the base stations.

In this section, the decentralized coordinated multicell beamforming algorithm has been introduced for solving the beamforming problem in (21), which is referred as SOCP algorithm throughout the next chapters. In Section 3.4.2 further analysis is carried out for characterizing the behavior of this algorithm in large antenna domain.

3.3.2. *Beamforming via uplink-downlink duality*

Uplink-downlink duality provides a link between downlink beamforming problem and uplink detection problem. Figure 5 shows a downlink channel and its dual uplink. It can be shown that for the scenario depicted by Figure 5, the sum power of the downlink beamforming problem and the uplink detection problem are the same, when the same sets of target SINRs are going to be satisfied [37]. In addition, there are some further relations between downlink and uplink problems which are useful for transferring the downlink problem into the dual uplink problem. The motivation is that uplink problems are generally easier to solve than downlink problems.

Authors in [16] and [17] relate the uplink-downlink duality to the duality principle in optimization theory. In fact, each primal problem has a dual in way that the optimal objective values for both of the primal and the dual problems are the same (zero duality gap) when the problem is feasible [34]. They show that the downlink beamforming problem defined by (21) (with the assumption that each user is served by a single base station) is a primal problem which has a dual given by (31). The solution of the dual problem gives the uplink powers and detection vectors,

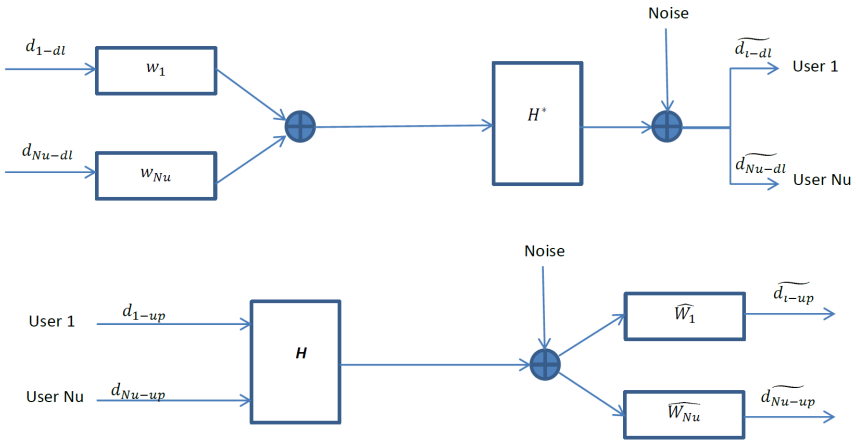

Figure 5: Linear Uplink-downlink duality

$$\begin{aligned} \underset{\hat{\mathbf{w}},\lambda}{\text{minimize}} \quad & \sum_{b\in\mathcal{B}}\sum_{k\in\mathcal{U}_b} \lambda_k N_0 \\ \text{subject to} \quad & \frac{\lambda_k |\hat{\mathbf{w}}_{b_k,k}^H \mathbf{h}_{b_k,k}|^2}{\sum_{l\neq k} \lambda_l |\hat{\mathbf{w}}_{b_l,l}^H \mathbf{h}_{b_l,k}| + |\hat{\mathbf{w}}_{b_k,k}|^2} \geq \gamma_k \ \forall k \in \mathcal{U}, \end{aligned} \tag{31}$$

The optimization variables for the dual problem are $\hat{\mathbf{w}}_{b,k}$ and λ_k which can be also interpreted from the uplink-downlink duality point of view. In other words, the optimal $\hat{\mathbf{w}}_{b,k}$ is the detection vector of the dual uplink channel and $\lambda_k N_0$ is the transmit power of the k^{th} user. The duality principle in optimization theory and uplink-downlink duality well define each other, i.e the optimal value for (31) is the same as the optimal value of (21) which relates the downlink and the uplink power allocations.

Now, the question is that how to solve the dual uplink problem? For the problem in (31) , it is well known that the optimal detection vector $\hat{\mathbf{w}}_{b,k}$ that maximizes the SINR value, under the fixed power assumption, is the minimum mean square error receiver [3]. Thus, $\hat{\mathbf{w}}_{b,k}$ is given by,

$$\hat{\mathbf{w}}_{b_k,k} = (\sum_{l} \lambda_l \mathbf{h}_{b_k,l} \mathbf{h}_{b_k,l}^H + I)^{-1} \mathbf{h}_{b_k,k} \tag{32}$$

Without loss of generality, N_0 is assumed equal to one. Moreover, authors in [17] shows that the optimal uplink power allocation can be achieved by a fixed point iteration formula,

$$\lambda_k = \frac{1}{(1+\frac{1}{\gamma_k})\mathbf{h}_{b_k,k}^H (I + \mathbf{\Sigma}_{b_k})^{-1} \mathbf{h}_{b_k,k}} \tag{33}$$

$$\mathbf{\Sigma}_b = \sum_{l \in \mathcal{U}} \lambda_k \mathbf{h}_{b,l} \mathbf{h}_{b,l}^H \tag{34}$$

To sum up, the dual uplink problem solver iterates (33) for obtaining the optimal uplink powers. Then, the optimal detection vectors result from (32). Unlike the primal problem, the dual problem does not require convex optimization tools.

Now the question is that how the optimal power allocation and beamformer for the downlink problem can be achieved based on the results of the uplink problem? Work in [17] answers this question by providing a connection between the optimal downlink beamformer and the dual uplink detection vectors,

$$\mathbf{w}_{b_k,k} = \sqrt{\delta_k} \hat{\mathbf{w}}_{b_k,k} \tag{35}$$

where, $\mathbf{w}_{b,k}$ is the downlink beamformer for the k^{th} user and δ_k can be found by using the following matrix inversion [16], [20],

$$G_{i,j} = \begin{cases} \frac{1}{\gamma_i} |\hat{\mathbf{w}}_{b_i,i}^H \mathbf{h}_{b_i,i}|^2 & i = j \\ -|\hat{\mathbf{w}}_{b_j,j}^H \mathbf{h}_{b_j,i}|^2 & i \neq j \end{cases} \tag{36}$$

Then,

$$\boldsymbol{\delta} = \mathbf{G}^{-1} \mathbf{1}_{Nu} \tag{37}$$

where, $\boldsymbol{\delta}$ is a vector that contains all δ_k values and $\mathbf{1}_{Nu}$ is a $Nu \times 1$ vector with all elements equal to one.

The above set of equations, defines an algorithm which gives the optimal power allocation and beamformers for the downlink (21) and uplink (31) problems. The results are derived based on the uplink-downlink duality which is well related with the duality concept in optimization theory.

3.4. Large dimension approximation

The solutions that have been studied in the previous sections require exchange of some information among the cooperating nodes which makes their real time deployment

difficult, if not impossible. The channel realizations change very rapidly, thus, a real time beamforming solution should converge very rapidly in order to cope with the varying nature of the problem. When dimensions of the problem are large, the channel fading becomes averaged out. Therefore, dependency of the optimal solution on the instantaneous channel realizations decreases which result in a simpler solution with a smaller rate of information exchange among the cooperating nodes.

Large dimension approximations allow utilizing this averaging property for proposing a simpler solution. Authors in [20] have studied a large dimension approximation for the beamforming method based on the uplink-downlink duality. The results of this study are presented in Section 3.4.1. They show that the algorithm can decide about the optimal beamformer based on statistics of channel which results in a simpler solution with lower exchange rate. However, the error of this approximation is translated into a deviation of the resulted SINR from the target QOS.

The other approach based on the SOCP algorithm is the focus of the study in this thesis work. In Section 3.4.2, the large dimension behavior of the SOCP algorithm is investigated. The results allow prediction of the optimal intercell interference (the parameter that couples the sub-problems) based on statistics of channel which result in decoupling of the subproblems at base stations. The error in the approximations does not affect the SINRs, but causes a higher transmit power than the exact solution. In addition, it is inferred from the results that the SOCP algorithm in the large dimensions regime requires a smaller amount of information exchange inherently.

3.4.1. Large dimension approximation for uplink-downlink duality

The algorithm defined by (33) and (32) is based on the fixed point iteration that has a fast convergence rate and a simple structure for implementation. However, it is argued in [20] that this algorithm requires exchange of instantaneous CSI between base stations which is not desired for a realtime deployment, especially when dealing with a fast fading scenario. Therefore, authors in [20] propose reducing the dependency on instantaneous CSI by providing a large dimension approximation for (33) and (36). The result is a simpler solution that depends just on statistics of channel; nevertheless, the target SINRs cannot be guaranteed because of the approximations.

Consider the system model defined in Section 3.1 and let $Nu \rightarrow \infty$, while $\frac{N_{\mathrm{a}}}{Nu} \rightarrow \mathrm{cte}$. The channel vectors are assumed to be Gaussian distributed with independent entries $\mathbf{h}_{b,k} \sim \mathbb{CN}(0, a_{b,k}\mathbf{I}_{\mathrm{N_a}})$, the variance of which depends on the path losses from the BSs to the users. Under these assumptions, it is shown in [20] that the large dimension approximation for (33) is given by:

$$\lambda_k = ((1 + \frac{1}{\gamma_k})(\frac{a_{b_k,k}^2 m_{\mathbf{\Sigma}_{b_k}}(-1)}{1 + a_{b_k,k}^2 \lambda_k m_{\mathbf{\Sigma}_{b_k}}(-1)}))^{-1} \tag{38}$$

Where, $a_{b_k,k}^2$ is the pathloss from the k^{th} user to its serving base station. $\mathbf{\Sigma}_{b_k}$ is defined by (34) and $m_{\mathbf{\Sigma}_{b_k}}(-1)$ is the Stieltjes transform of the Gram matrix $\mathbf{\Sigma}_{b_k}$ at point $z = -1$. More details about large dimension approximation and Stieltjes transform are presented in appendix A. Nevertheless, what is important here is that the Stieltjes transform of $\mathbf{\Sigma}_{b_k}$ just depends on the channel statistics and not on the instantaneous

CSI. Thus the rate of data exchange among the base stations reduces significantly. Moreover, even in a fast fading scenario, the channel statistics do not change very rapidly. Therefore, the base stations calculate λ_k based on the statistics of the channel. Then $\hat{\mathbf{w}}_{b_k,k}$ can be found by using (32) and based on the local CSI.

Similarly, a large dimension approximation for (36) is given by [20],

$$G_{i,j} = \begin{cases} \frac{1}{\gamma_i}\left(\frac{a_{b_i,i}^2 m_{\mathbf{\Sigma}_{b_i}}(-1)}{\eta_{b_i,i}}\right)^2 & i = j \\ \frac{-1}{N_{\mathrm{a}}} \frac{a_{b_j,i}^2 a_{b_j,j}^2 m'_{\mathbf{\Sigma}_{b_j}}(-1)}{\eta_{b_j,i}^2 \eta_{b_j,j}^2} & i \neq j \end{cases} \tag{39}$$

$$\eta_{b_j,i} = 1 + a_{b_j,i}^2 \lambda_i m_{\mathbf{\Sigma}_{b_j}}(-1) \tag{40}$$

where, $m'_{\mathbf{\Sigma}_b}(-1)$ is the differential of $m_{\mathbf{\Sigma}_b}(z)$ with respect to z at point $z = -1$ (see appendix A, Theorem A-2).

The algorithm defined by these approximations can be implemented in a distributed manner and it just needs the statistics of the channel to be exchanged.

One might argue about the validity of the large dimension approximations for the practical scenarios where the dimensions do not go to infinity. As discussed earlier, results of random matrix theory provide good approximations even for finite dimensions. The simulation carried out by [20] shows that even for 50 users and 50 antennas at the base stations, the algorithm gives a good approximation. Nevertheless, the achieved SINR values in the simulations are different from the target SINR.

3.4.2. Characterizing large dimension behaviors of SOCP algorithm

The simulations in Chapter 4 show that in a network with practically large antenna arrays at BSs, the optimal methods like the SOCP algorithm outperform other suboptimal algorithms like ZF and MF. Even though, these simulations did not take into account all practical limitations; but, the results give the motivation for working on application of an optimal solutions like the SOCP algorithm in the large antennas domain. Thus, the coming sections are devoted to the efforts in characterizing the SOCP algorithm behaviors and proposing possible simplifications in large antenna regime. The study starts by characterizing the parameter that couples the subproblems, i.e intercell interference. The results allow prediction of the optimal intercell interference based on the statistics of the channel. This predictable behavior of the intercell interference in the large dimension regime suggests an strategy for decoupling the subproblems. In addition, some further properties for intercell interference in the large dimension region are extracted.

Large dimension approximation for intercell interference

Investigating the role of intercell interference seems a good starting point for the large dimension characterization of the SOCP algorithm. This parameter couples subproblems at base stations, i.e it obliges the coupled base stations to exchange their corresponding intercell interference terms. In addition, the SOCP algorithm as described in Chapter 3, relies on an iterative solution, i.e it solves the subproblems after each

exchange. Therefore, intercell interference not only defines the required backhaul signaling, but it also affects the complexity of the solution, which justifies the efforts in studying its behavior.

Looking at (27) in Section 3.3.1, it is clear that the intercell interference from all the base stations towards user k is,

$$ICI_k = \sum_{b \in \overline{\mathcal{B}_k}} \sum_{l \in \mathcal{U}_b} |\mathbf{h}_{b,k}^H \mathbf{w}_{b,l}|^2 \tag{41}$$

Then, the intercell interference term from the bth base station to user k is,

$$ICI_{b,k} = \sum_{l \in \mathcal{U}_b} |\mathbf{h}_{b,k}^H \mathbf{w}_{b,l}|^2 \tag{42}$$

Looking at (35), the intercell interference term in (42) can be written as follows,

$$ICI_{b,k} = \sum_{l \in \mathcal{U}_b} \sqrt{p_{b,l}} \frac{|\hat{\mathbf{w}}_{b,l}^H \mathbf{h}_{b,k}|^2}{|\hat{\mathbf{w}}_{b,l}|^2} \tag{43}$$

where, $p_{b,l}$ is the downlink power that the b^{th} BS assigned to the l^{th} user. $\hat{\mathbf{w}}_{b,l}$ is the uplink detector vector defined by (32). Expanding $\hat{\mathbf{w}}_{b,l}$ gives,

$$\begin{aligned} ICI_{b,k} &= \sum_{l \in \mathcal{U}_b} \frac{p_{b,l}}{|\hat{\mathbf{w}}_{b,l}|^2} \mathbf{h}_{b,k}^H \hat{\mathbf{w}}_{b,l} \hat{\mathbf{w}}_{b,l}^H \mathbf{h}_{b,k} \\ &= \sum_{l \in \mathcal{U}_b} p_{b,l} \frac{\mathbf{h}_{b,k}^H (\mathbf{\Sigma}_b + N_0 I)^{-1} \mathbf{h}_{b,l} \mathbf{h}_{b,l}^H (\mathbf{\Sigma}_b + N_0 I)^{-1} \mathbf{h}_{b,k}}{|\hat{\mathbf{w}}_{b,l}|^2} \end{aligned} \tag{44}$$

This structure of the intercell interference allows derivation of a large dimension approximation based on the lemmas presented in appendix A. At first, Lemma A-2 (matrix inversion lemma) is applied to the numerator of (44) which makes the matrix $\mathbf{\Sigma}_b$ independent of $\mathbf{h}_{b,k}$,

$$\begin{aligned} ICI_{b,k} &= \sum_{l \in \mathcal{U}_b} \frac{p_{b,l}}{|\hat{\mathbf{w}}_{b,l}|^2} \left(\frac{\mathbf{h}_{b,k}^H (\mathbf{\Sigma}_b^{/k} + I)^{-1} \mathbf{h}_{b,l} \mathbf{h}_{b,l}^H (\mathbf{\Sigma}_b^{/k} + I)^{-1} \mathbf{h}_{b,k}}{(1 + \lambda_k \mathbf{h}_{b,k}^H (\mathbf{\Sigma}_b^{/k} + I)^{-1} \mathbf{h}_{b,k})^2} \right) \\ &= \sum_{l \in \mathcal{U}_b} \frac{p_{b,l}}{|\hat{\mathbf{w}}_{b,l}|^2} \left(\frac{a_{b,k}^2 N_{\text{a}} \hat{\mathbf{h}}_{b,k}^H \mathbf{T}_{b,l} \hat{\mathbf{h}}_{b,k}}{(1 + \lambda_k a_{b,k}^2 N_{\text{a}} \hat{\mathbf{h}}_{b,k}^H (\mathbf{\Sigma}_b^{/k} + I)^{-1} \hat{\mathbf{h}}_{b,k})^2} \right) \end{aligned} \tag{45}$$

$$\mathbf{T}_{b,l} = (\mathbf{\Sigma}_b^{/k} + I)^{-1} \mathbf{h}_{b,l} \mathbf{h}_{b,l}^H (\mathbf{\Sigma}_b^{/k} + I)^{-1} \tag{46}$$

$$\hat{\mathbf{h}}_{b,k} = \frac{\mathbf{h}_{b,k}}{a_{b,k} \sqrt{N_{\text{a}}}} \tag{47}$$

$$\mathbf{\Sigma}_b^{/k} = \mathbf{\Sigma}_b - \lambda_k \mathbf{h}_{b,k} \mathbf{h}_{b,k}^H \tag{48}$$

Without loss of generality, N_0 is assumed to be equal to one, which makes the notations simpler. In addition, The pathloss gain $a_{b,k}^2$ is taken out of $\mathbf{h}_{b,k}$ which prepares

(45) for applying Lemma A-3. Thus, $\hat{\mathbf{h}_{b,k}}$ is the normalized channel with respect to the pathloss and the number of antennas.

Looking at (45), it can be seen that matrix $\mathbf{T}_{b,l}$ and $(\mathbf{\Sigma}_b^{/k} + I)^{-1}$ at the numerator and the denominator are independent of $\hat{\mathbf{h}}_{b,k}$. Moreover, the other conditions specified by Lemma A-3 are satisfied. Therefore, Lemma A-3 can be applied to both of the numerator and the denominator of (45) that gives,

$$ICI_{b,k} = \sum_{l \in \mathcal{U}_b} \frac{p_{b,l} a_{b,k}^2}{|\hat{\mathbf{w}}_{b,l}|^2} \left(\frac{tr[\mathbf{T}_{b,l}]}{\left(1 + \lambda_k a_{b,k}^2 tr[(\mathbf{\Sigma}_b^{/k} + I)^{-1}]\right)^2} \right) \tag{49}$$

Based on the result of Lemma A-4 (Rank-1 perturbation lemma), $tr[(\mathbf{\Sigma}_b^{/k} + I)^{-1}]$ can be replaced with $tr[(\mathbf{\Sigma}_b + I)^{-1}]$. Moreover, Theorem A-2 says that the difference between $\frac{1}{N_\mathrm{a}} tr[(\mathbf{\Sigma}_b + I)^{-1}]$ and $m_{\mathbf{\Sigma}_b}(-1)$ goes to zero as the dimensions grow large, where, $m_{\mathbf{\Sigma}_b}(-1)$ is the stieltjes transform of $\mathbf{\Sigma}_b$ at point $z = -1$. Thus, (49) can be rewritten as,

$$\begin{aligned} ICI_{b,k} &= \sum_{l \in \mathcal{U}_b} \frac{p_{b,l} a_{b,k}^2}{|\hat{\mathbf{w}}_{b,l}|^2} \left(\frac{tr[\mathbf{T}_{b,l}]}{\left(1 + \lambda_k a_{b,k}^2 N_\mathrm{a} m_{\mathbf{\Sigma}_b}(-1)\right)^2} \right) \\ &= \sum_{l \in \mathcal{U}_b} \frac{p_{b,l} a_{b,k}^2}{|\hat{\mathbf{w}}_{b,l}|^2} \left(\frac{tr[\mathbf{T}_{b,l}]}{\psi_{b,k}^2} \right) \end{aligned} \tag{50}$$

$$\psi_{b,k} = 1 + \lambda_k a_{b,k}^2 N_\mathrm{a} m_{\mathbf{\Sigma}_b}(-1) \tag{51}$$

Theorem A-2 defines a system of equations that gives the $m_{\mathbf{\Sigma}_b}(-1)$ based on the statistics of the channels.

In the Next step, $|\hat{\mathbf{w}}_{b,l}|^2$ term at the denominator of (50) is expanded,

$$ICI_{b,k} = \sum_{l \in \mathcal{U}_b} \frac{p_{b,l} a_{b,k}^2}{\psi_{b,k}^2} \cdot \frac{tr(\mathbf{\Sigma}_b^{/k} + I)^{-1} \mathbf{h}_{b,l} \mathbf{h}_{b,l}^H (\mathbf{\Sigma}_b^{/k} + I)^{-1}}{\mathbf{h}_{b,l}^H (\mathbf{\Sigma}_b + N_0 I)^{-1} (\mathbf{\Sigma}_b + N_0 I)^{-1} \mathbf{h}_{b,l}} \tag{52}$$

From properties of trace, it is known that [38],

$$tr(c) = c, \; c \text{ is scalar} \tag{53}$$

$$tr(\mathbf{ABC}) = tr(\mathbf{BCA}) = tr(\mathbf{CAB}) \tag{54}$$

Using these lemmas, (52) can be rearranged as follows,

$$ICI_{b,k} = \sum_{l \in \mathcal{U}_b} \frac{p_{b,l} a_{b,k}^2}{\psi_{b,k}^2} \cdot tr \left(\frac{\mathbf{h}_{b,l}^H (\mathbf{\Sigma}_b^{/k} + I)^{-1} (\mathbf{\Sigma}_b^{/k} + I)^{-1} \mathbf{h}_{b,l}}{\mathbf{h}_{b,l}^H (\mathbf{\Sigma}_b + N_0 I)^{-1} (\mathbf{\Sigma}_b + N_0 I)^{-1} \mathbf{h}_{b,l}} \right) \tag{55}$$

Finally, by applying Lemma A-4.(Rank-1 perturbation lemma) to the numerator of (55), the terms in the numerator and the denominator cancel each other. Therefore,

the large dimension approximation for the intercell interference term from the b^{th} base station to the k^{th} user can be written as,

$$\begin{aligned} ICI_{b,k} &= \sum_{l \in \mathcal{U}_b} \frac{p_{b,l} a_{b,k}^2}{\psi_{b,k}^2} \\ &= \frac{a_{b,k}^2}{(1 + \lambda_k a_{b,k}^2 N_{\text{a}} m_{\mathbf{\Sigma}_b}(-1))^2} \sum_{l \in \mathcal{U}_b} p_{b,l} \end{aligned} \tag{56}$$

Based on this result, the large dimension behavior of the optimal intercell interference can be studied. In this equation the stieltjes transformation just depends on the channel statistics, also λ as defined by (38) is determined by the statistics of the channel. Thus, when the dimensions of the system are large enough, the intercell interference is defined by the statistics of the channel. This point indicates that the optimal intercell interference calculated using (27) is valid for several symbol intervals (because the statistics of the channel do not change very rapidly). Therefore, the required inter base station exchange rate is inherently smaller in a system with large dimensions.

Another interesting point is that the intercell interference term depends directly on $a_{b,k}^2 \sum_{l \in \mathcal{U}_b} p_{b,l}$, which is indeed a true statement. The more power the b^{th} base station injects into the antennas, the more interference that is emitted to other users. This point supports the minimum power beamforming method. In fact this method satisfies the user's SINRs with a minimum transmit power, which results in a smaller interference even to the possible non-coordinated users. The existence of the pathloss is clear because it weakens the transmitted signal throughout the propagation path. Therefore, the users do not suffer substantially from the far interfering source. This is a trick that the optimal beamforming methods utilize, as discussed in Section 4.1. In addition to $a_{b,k}^2 \sum_{l \in \mathcal{U}_b} p_{b,l}$, there are some other parameters in the denominator of (56) which modify the raw approximation ($a_{b,k}^2 \sum_{l \in \mathcal{U}_b} p_{b,l}$) by taking into account some other parameters.

In addition to the above characterizations, a procedure can be proposed for decoupling the subproblems in the SOCP algorithm. The optimal intercell interference terms (the coupling parameters) can be predicted based on the statistics of the channel. Once the optimal intercell interference is achieved, it is possible to solve the subproblems independently. Thus, the suggested decentralized algorithm for approximating the optimal ICI can be written as follows, which provides a decoupling procedure for the optimization problem defined by (27).

1. Exchange the channel statistics (the path losses) between the base stations.
2. Initialize the λ values.
3. Calculate $m_{\mathbf{\Sigma}_b}(-1)$ and $m'_{\mathbf{\Sigma}_b}(-1)$ at each base station based on the results of Theorem A-2.
4. Calculate the optimal λ values by using the large dimension approximation defined by (38).
5. Return to step 3 and repeat these steps until the convergence of the optimal λ and $m_{\mathbf{\Sigma}_b}$.

6. Calculate the large dimension approximation of the optimal p values using (39).
7. Finally get the large dimension approximation of the optimal intercell interference using (56).

The optimal intercell interference resulted from this algorithm is valid until a change occurs in the statistics of the channels. Therefore, the optimal ICI in the large dimension regime is valid for several symbol intervals, even for a fast fading scenario.

In this section a large dimension approximation has been derived for the optimal intercell interference term based on the optimization problem defined by (27). This approximation makes it possible to study the behavior of this parameter when the dimensions of the problem grow large. In addition an algorithm has been derived that approximates the optimal intercell interference based on the channel statistics that results in decoupling of the subproblems in the SOCP algorithm.

3.5. Summary and discussion

In this chapter, the minimum power beamforming problem has been introduced and two different solutions have been proposed. In addition, a large dimension approximation for the uplink-downlink duality method has been reviewed and the advantages and the disadvantages of this approximation were studied. Moreover, by following the same procedure, a large dimension approximation for intercell interference term (as the coupling term for the subproblems of the SOCP algorithm) has been derived which resulted in proposal of a procedure for decoupling the subproblems of the SOCP algorithm.

The next chapter presents the simulation results. The simulations study the performance of the SOCP algorithm compared to other sub-optimal methods like ZF and MF over a wide range of the number of antennas. Also the validity of the large dimension approximation for the intercell interference term is examined based on simulations.

4. RESULTS

In Chapter 3, the problem of interest and the system model have been defined and possible solutions have been reviewed. In this chapter the SOCP solution is considered as the benchmark. The focus is on characterizing the behavior of this algorithm when dimensions of the problem grow large. Also, other downlink beamforming methods are considered and differences in performance of these algorithms are studied. The system model considered here is the same as the model defined in Section 3.1; nevertheless, it is assumed that each stream is transmitted from a single base station.

In addition to various beamforming methods, two different user allocation strategy are considered. The first one assigns the users to their nearest base station while the other approach performs an exhaustive search over all possible assignments for finding the best one (BS assignment). The later approach provides a large gain for the users on the cell edges; however, this scheme requires a centralized processing [19]. Under each of these user allocation strategies, following methods are compared using simulation:

- Minimum power beamforming based on SOCP algorithm, introduced in Chapter 3.
- Zero forcing where the beamformers are defined by [19]:

$$[\mathbf{w}_{b,1}, ..., \mathbf{w}_{b,4}] = \mathbf{H}_b^{\mathbf{H}}(\mathbf{H}_b\mathbf{H}_b^H)^{-1} \tag{57}$$

  where,

$$\mathbf{H}_b = [\mathbf{h}_{b,1}, ..., \mathbf{h}_{b,4}]^T, b = 1, 2 \tag{58}$$

- MF beamforming:

$$\mathbf{w}_{b,i} = \frac{\mathbf{h}_{b,i}}{|\mathbf{h}_{b,i}|}, b = 1, 2, i \in \mathcal{U}_b \tag{59}$$

In MF beamforming method, the transmit power is adjusted such that the target SINRs become satisfied under an orthogonal channel assumption.

4.1. Simplified system model

As a starting point a simplified system model is considered (the same as [19]). There are 4 single antenna users which are served by 2 base stations. The number of antennas at the base stations varies from 4 up to 120. It is assumed that user 1 and user 2 (3 and 4) have a shorter distance to the first BS (second BS). However, those are not obliged to be served by their nearest BS. All users have identical pathlosses with respect to their nearest base stations i.e. $a_{1,1} = a_{1,2} = a_{2,3} = a_{2,4} = a$ ($a_{b,k}^2$ is the pathloss from the b^{th} base station to the k^{th} user). The distance between the user's groups is defined by parameter $\alpha = \frac{a_{1,1}^2}{a_{1,3}^2} = \frac{a_{2,3}^2}{a_{2,1}^2}$. Without loss of generality N_0 is assumed to be equal to one. Figure 6 shows this scenario.

In the coming sections, an ideal scenario with i.i.d channel entries and a non-ideal scenarios with correlation among channel entries are considered and the observations with different number of antennas are analyzed.

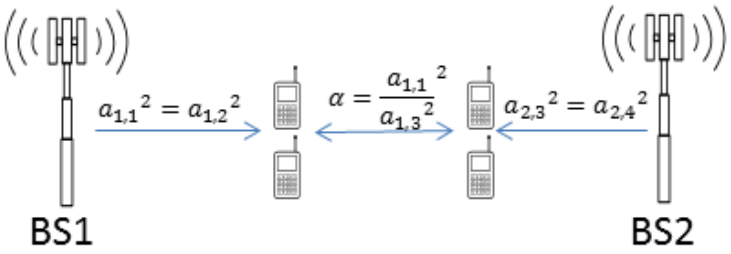

Figure 6: A simplified model with two base stations.

4.1.1. Ideal scenario

In the ideal scenario the channels are i.i.d and Gaussian distributed with zero mean and variance defined by the path losses. Therefore, there is no correlation between the antenna elements or between the user's channels. This is the ideal channel which has the desired conditions for the massive MIMO operation (as discussed in Chapter 2). Thus all the different methods should converge to the same performance when the number of antennas at BS increases. Figures 7 to 12 depict the total transmit power required for satisfying a set of target SINRs as a function of the number of antennas at the base stations. Figures differ in target SINR and distance between users group. When users are on the cell edge, the α value is 0dB and it increases when the user's groups are further apart. The correlation coefficient between the channel entries (ν) is equal to zero for all figures in the ideal scenario; however, some more realistic cases with correlation is considered in the next section.

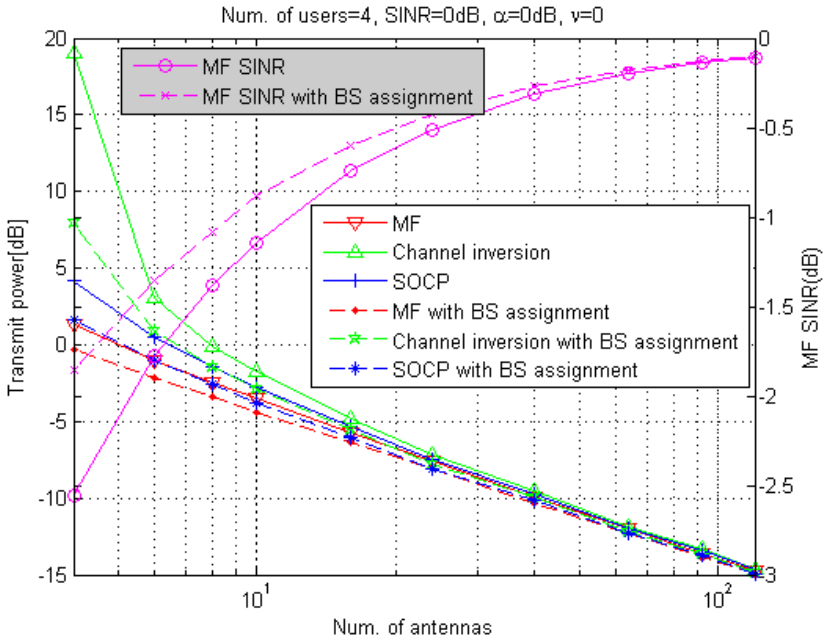

Figure 7: Transmit power versus num. of antennas, SINR= 0dB, α= 0dB.

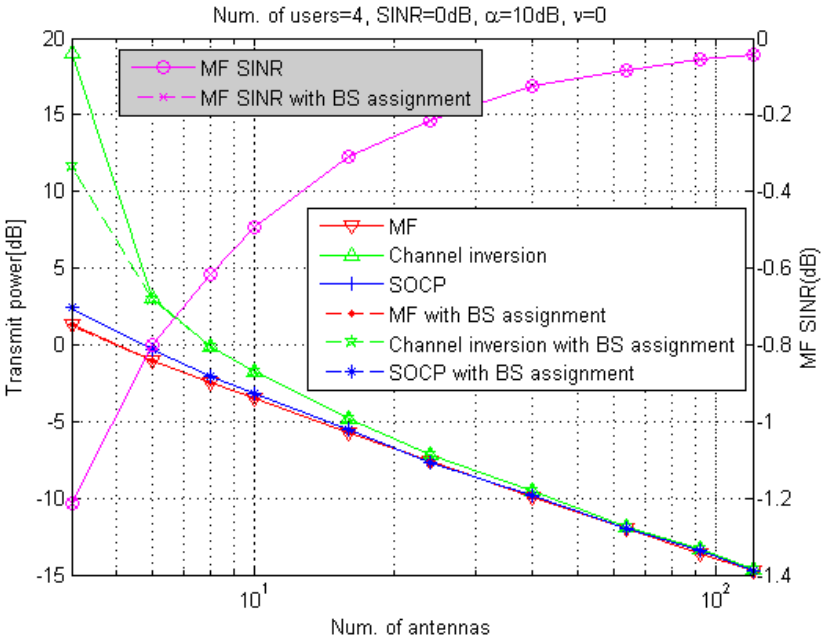

Figure 8: Transmit power versus num. of antennas, SINR= 0dB, α= 10dB.

As anticipated, all the methods converge to the same performance when the number of antennas increases. This is predicted by the theories reviewed in Chapter 2. Another interesting point is the rate of convergence. All the methods almost converge when the number of antennas is greater than 20. This indicates the validity of the large dimension approximations (discussed in Chapter 2) for an i.i.d case with finite dimensions.

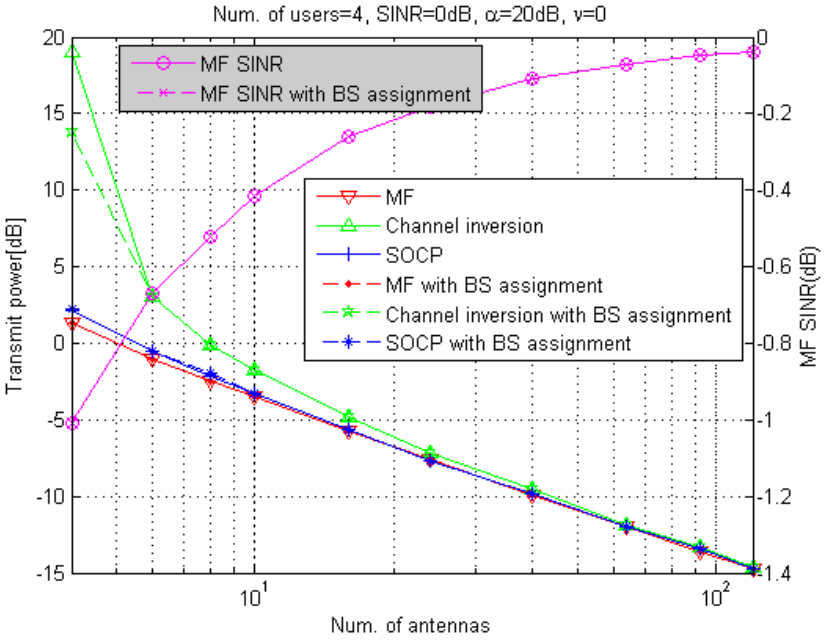

Figure 9: Transmit power versus num. of antennas, SINR= 0dB, α= 20dB.

Among the above mentioned methods, MF beamforming must be dealt with more care. The growing curve shows the resulted SINR when MF beamforming is used. When the number of antennas is small, the resulted SINR is well below the target SINR

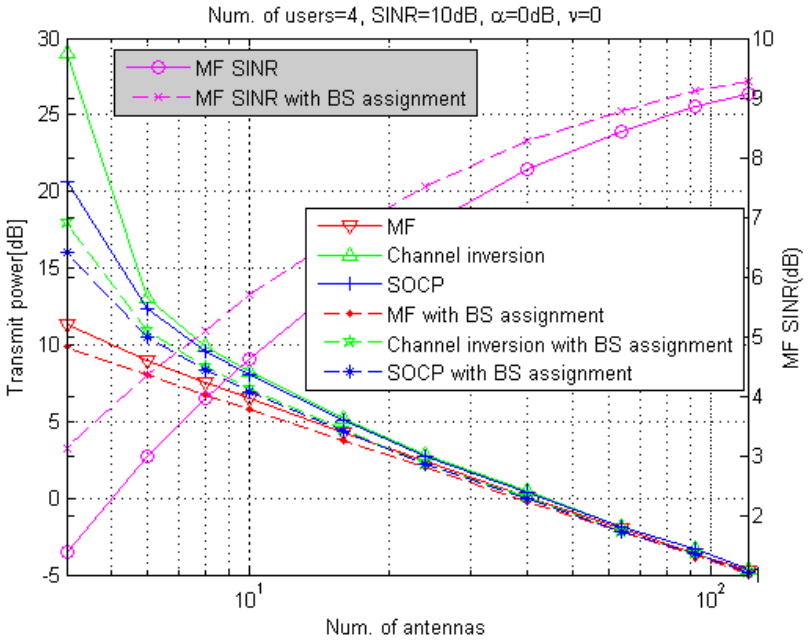

Figure 10: Transmit power versus num. of antennas, SINR= 10dB, α= 0dB.

and by increasing the number of antennas it approaches the target SINR. Nevertheless, it does not fulfill the target SINR even for 120 antennas at the base station. One can see that for more than 20 antennas at the BS, the transmitting powers for the SOCP algorithm and the MF beamforming are almost the same, but the MF beamforming fails to satisfy the target SINR, which proves the sub-optimality of MF beamforming.

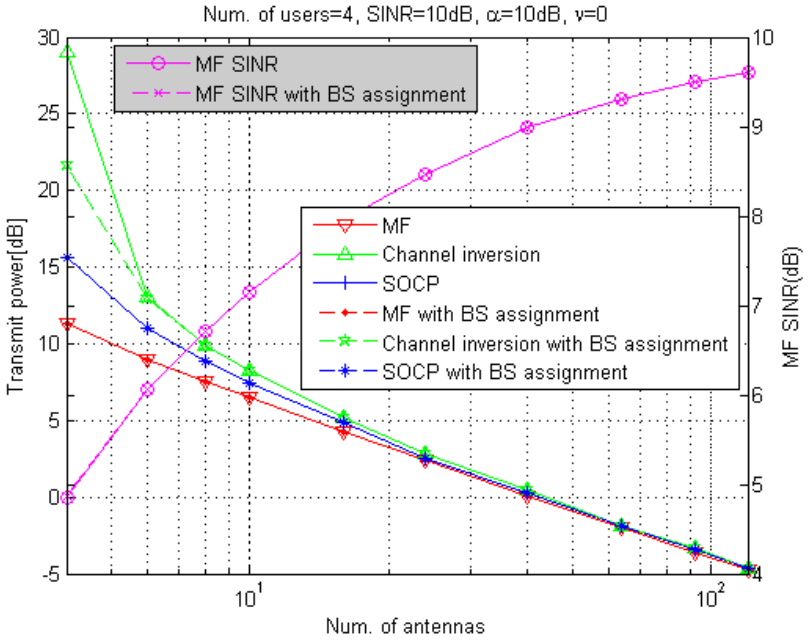

Figure 11: Transmit power versus num. of antennas, SINR= 10dB, α= 10dB.

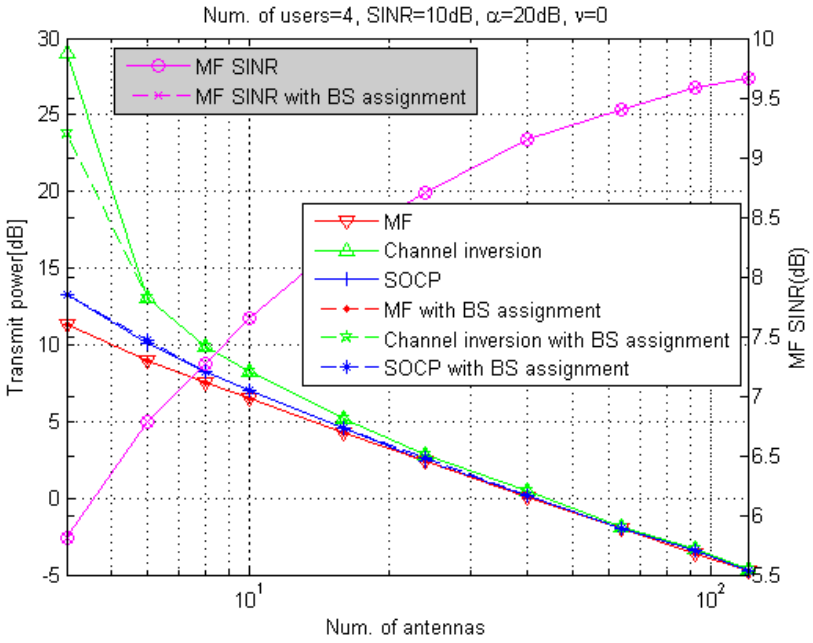

Figure 12: Transmit power versus num. of antennas, SINR= 10dB, α= 20dB.

When the number of antennas is smaller than 10, some interesting distinctions can be observed. The cell edge users enjoy substantial gains due to the fast user allocation, when an optimal user assignment is used. This gain is visible in Figure 7 and 10 ($\alpha = 0$dB). Therefore, there are some potential gains for distributed beamforming algorithms merged with distributed user assignment methods [19]. However, this difference diminishes for the number of antennas greater than 20 or when the user's groups are far from the cell edge. Also it is interesting that the optimal BS assignment provides a better SINR for the MF beamforming.

Another observation is related to the gap between the ZF and the SOCP algorithms without BS assignment. This gap is bigger when the users are near their serving cells. This is due to degradation of interference level when users go far from the interference source. In this situation the SOCP algorithm utilizes this opportunity, while the ZF algorithm wastes a d.o.f for nulling the interference toward the far users, which results in a performance difference. However, this gap is smaller between the corresponding cases with the BS assignment.

The gap of ZF and SOCP depends also on target SINR. For a fixed α value, incrementing the target SINR results in a smaller gap between ZF and SOCP. It is clear that for high target SINRs, the optimal strategy is reducing the level of interference, i.e following the same strategy as ZF, which results in the tendency of SOCP performance towards ZF one. The performance differences disappears even faster when the number of antennas increases.

In the results presented above, the number of users are constant. However, another interesting case is when the number of antennas and users grow with a fixed ratio. Figure 13 and 14 show the transmit power required for satisfying a target SINR, versus the number of antennas when $\frac{N_a}{N_u} = 4$. As can be seen, the SINR of MF beamforming degrades with increase of the number of antennas. The reason is the decrease of trans-

mit power required for satisfying a target SNR when the number of antennas increases, which results in a diminishing SINR. Note that for a set of orthogonal channels, the same transmit power can satisfy the target SINR. Thus, one can conclude that increasing the number of antennas and users with fixed ratio, does not result in orthogonality of channels, i.e the orthogonality channels is achieved only when the $\frac{N_{\mathrm{a}}}{N_{\mathrm{u}}}$ ratio goes to infinity.

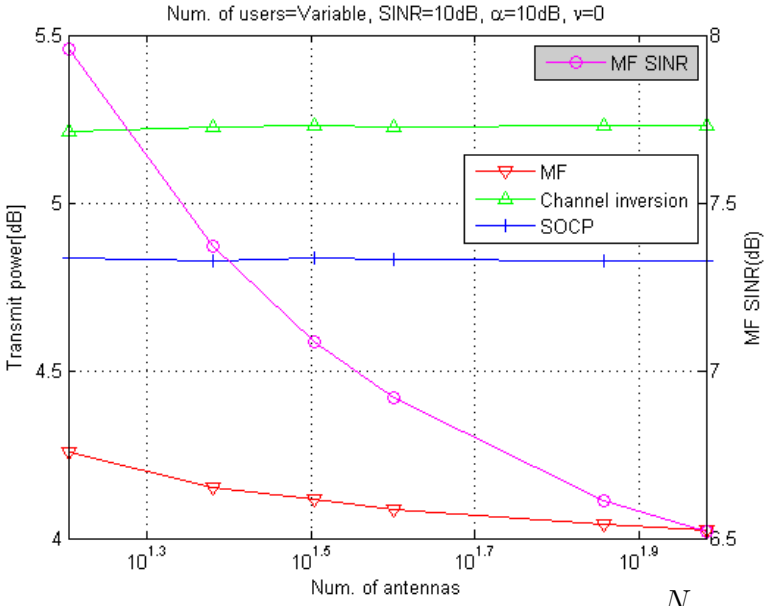

Figure 13: Transmit power versus num. of antennas, $\frac{N_{\mathrm{a}}}{N_{\mathrm{u}}} = 4$

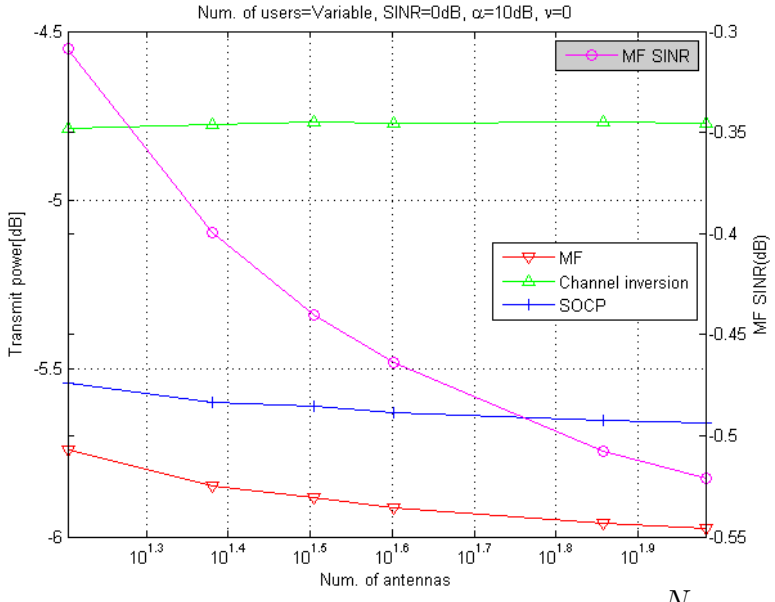

Figure 14: Transmit power versus num. of antennas, $\frac{N_{\mathrm{a}}}{N_{\mathrm{u}}} = 4$

In addition, the SINR of MF beamforming (see Section 2.5), when $N_{\mathrm{u}} \to \infty$ and $\frac{N_{\mathrm{a}}}{N_{\mathrm{u}}} = c$, is given by $\frac{\rho c}{\rho+1}$,where ρ is transmit power. For a fixed c value, this SINR

saturates with an error floor, as a function of SNR (ρ) [4]. Therefore, in this case, increasing the transmit power is not a good strategy for fulfilling the target SINRs.

On the other hand, looking at the ZF curve, the transmit power for ZF levels when the number of antennas increases. The SINR of ZF for large dimensions domain ($N_{\mathrm{u}} \to \infty$ and $\frac{N_{\mathrm{a}}}{N_{\mathrm{u}}} = c$) is given by $\rho(c-1)$ (see Section 2.5). Therefore, the power required for satisfying a target SINR remain fixed as a function of the number of antennas, when the c value is not changed, which is in line with the results of the simulation.

In this section an ideal simplified model has been considered which made it possible to examine the validity of the theories reviewed in Chapter 2. In the next sections some more realistic cases are considered.

4.1.2. Non-ideal scenario

In the non-ideal scenario, the Kronecker channel model [39] is used for introducing correlation between the antenna elements. It is assumed that the users are far from each other, thus there is no correlation between the user's channels. The system model is the same as in the previous section.

Results are depicted in Figures 15 to 20. These figures present the scenarios with two different correlation coefficient i.e. $\nu = 0.5, 0.9$.

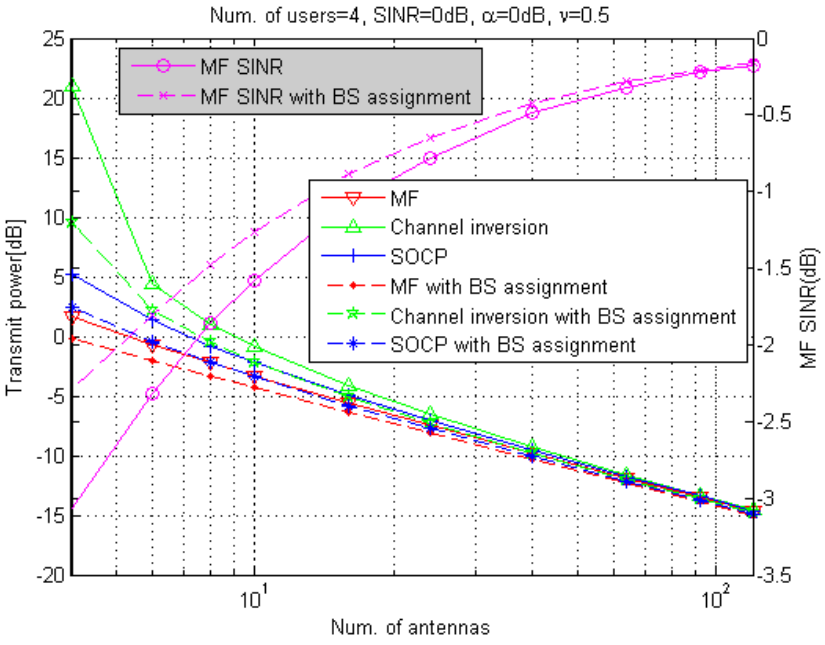

Figure 15: Transmit power versus num. of antennas, SINR= 0dB, α= 0dB, $\nu = 0.5$.

The first observation is the increased gap between different methods when the inter antenna element correlation increases. For example, in Figure 16, the transmit powers can be distinct even for the number of antennas equal to 50 (compare to Figure 7 with $\nu = 0$). Therefore, a larger antenna array is required for convergence of all the methods. Generally, correlation increases the gap between SOCP and ZF. Note that in

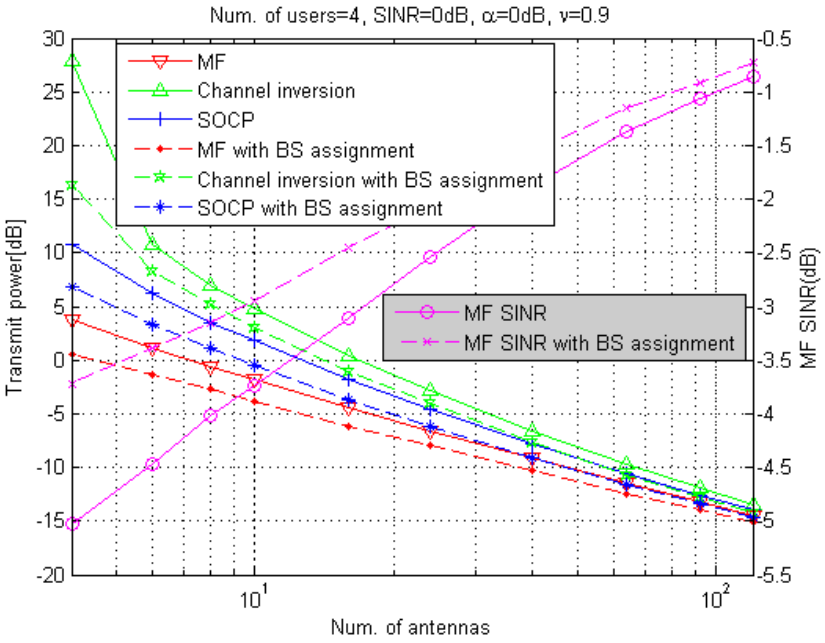

Figure 16: Transmit power versus num. of antennas, SINR= 0dB, α= 0dB, $\nu = 0.9$.

a correlated antenna array, efficient use of available d.o.f becomes more critical, thus the SOCP algorithm outperforms the ZF algorithm when the correlation coefficient increases.

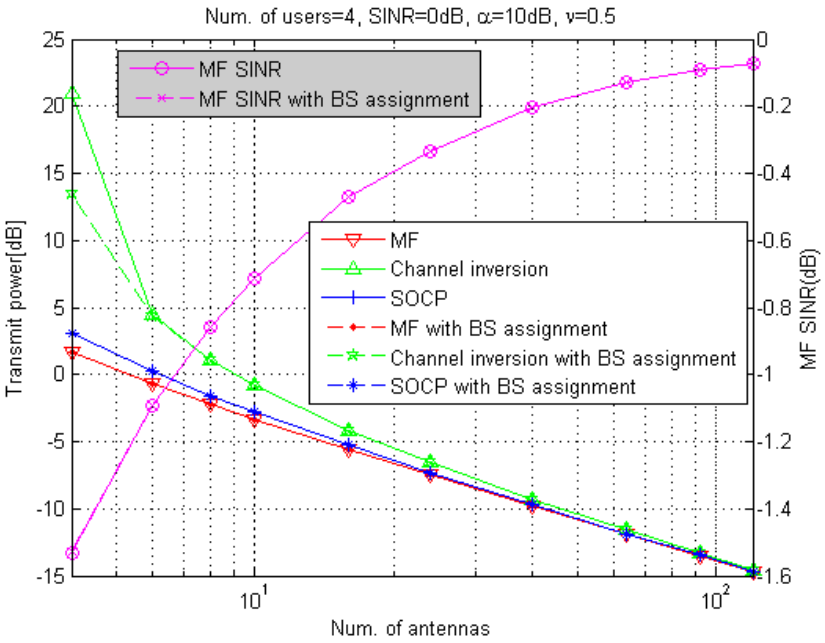

Figure 17: Transmit power versus num. of antennas, SINR= 0dB, α= 10dB, ν= 0.5.

Another interesting behavior is depicted by Figure 20, it can be seen that the gap between ZF and SOCP disappears when the antenna array grows large. However, the

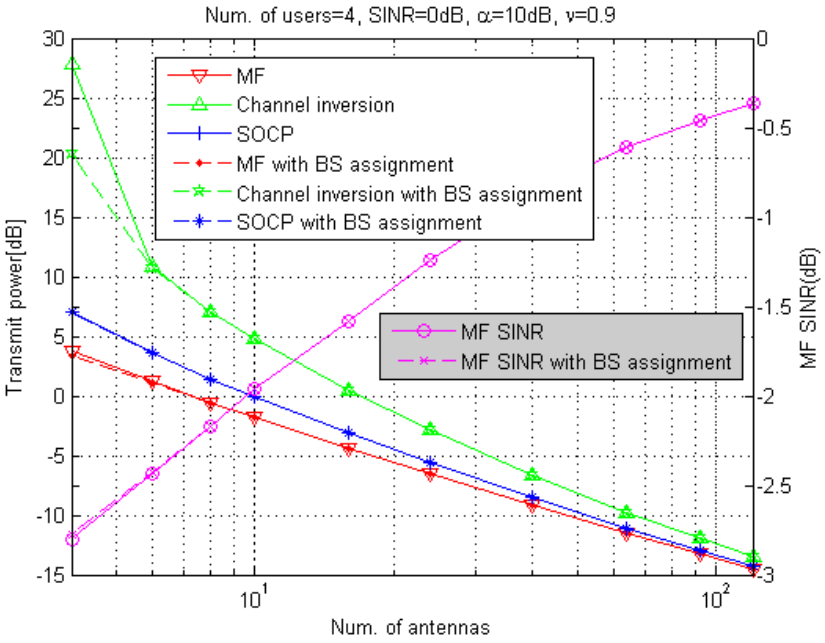

Figure 18: Transmit power versus num. of antennas, SINR= 0dB, α= 10dB, $\nu = 0.9$.

performance difference with respect to their corresponding methods with BS assignment remains visible for the cell edge users, which indicates the gains in optimal user allocation strategies merged with beamforming methods, even in a large dimension regime.

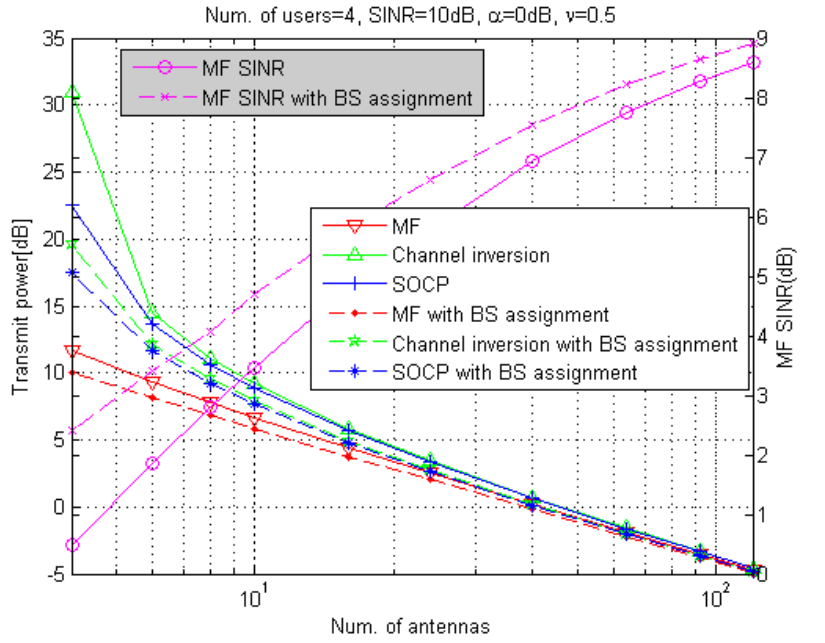

Figure 19: Transmit power versus num. of antennas, SINR= 10dB, α= 0dB, $\nu = 0.5$.

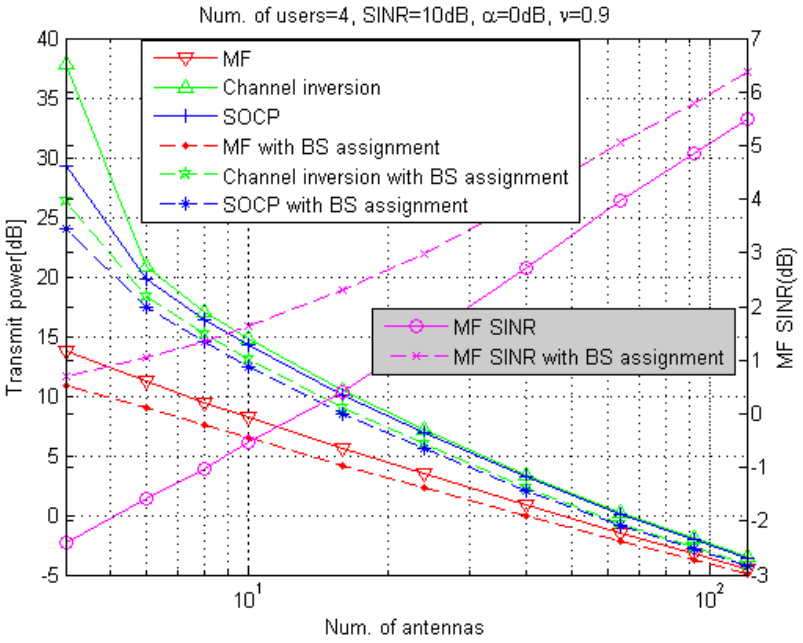

Figure 20: Transmit power versus num. of antennas, SINR= 10dB, α= 0dB, $\nu = 0.9$.

Finally, like in the i.i.d case, the MF beamforming is not successful in satisfying the target SINR even for 120 antennas. Note that the achieved SINR for the non-i.i.d case is smaller than the i.i.d case with the same number of antennas. For example the achieved SINR at 120 antennas in Figure 20 with $\nu = 0.9$ is 3dB less than the corresponding figure (Figure 10) with $\nu = 0$.

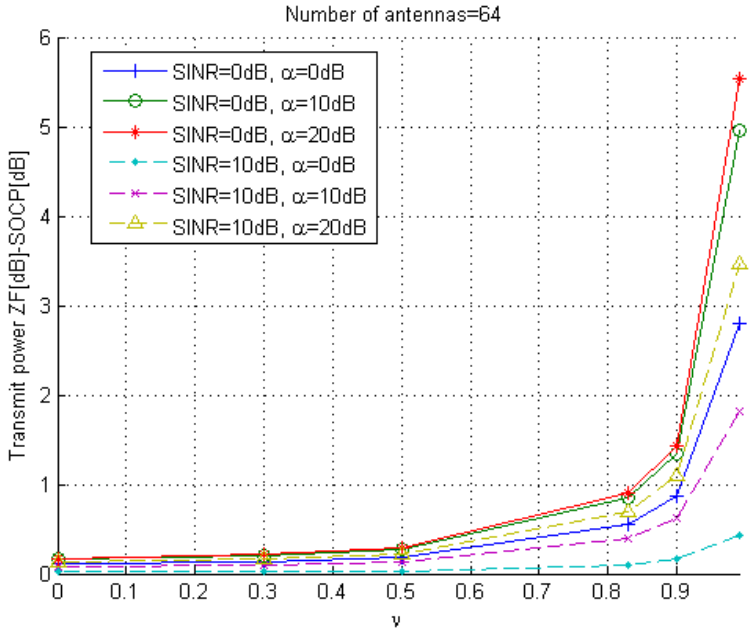

Figure 21: The gap between SOCP and ZF versus ν, $N_{\mathrm{a}} = 64$.

To sum up, it is observed that the correlation among the entries of the channels highlights the performance difference between the optimal and the sub-optimal methods. Figure 21 depicts the gap between the transmit power of SOCP and ZF as a function of correlation coefficient, when the number of antennas is equal to 64. It is clear that the difference grows when the correlation coefficient increases. However, as discussed before the gap is smaller when the target SINR is higher or when the users are on the cell edge (For example compare the curves with SINR=10dB and 0dB).

4.2. Network simulation

In this section a more realistic simulation is implemented. A network with 7 cells is considered and 28 users are scattered on the coverage area of the network, in a way that each cell contains 4 users. The same system model as in Chapter 3 is considered for the simulations; however, it is assumed that each user is served with a single base station. Exponential pathloss model is used for assigning the pathloss to each user. The pathloss exponent is 3 and the reference distance is 1m. The pathloss from a base station to the boundary of the reference distance of the neighboring base station is 50dB. The Kronecker channel model is used for introducing correlation between the antenna elements at the base stations. However, there is no correlation between the user's channels, because the users are assumed to be far enough from each other. The users are dropped randomly for each trial and in total 1000 trial are used for calculating the average transmit power. Figure 22 depicts this scenario.

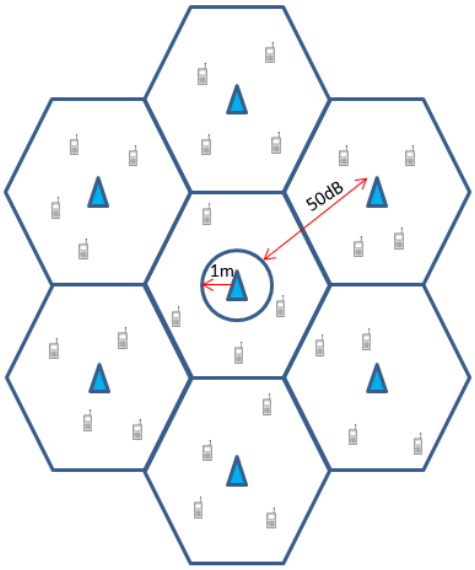

Figure 22: A Network with 7 Cells

The results of the simulation are shown in Figures 23 to 26. The correlation coefficients used for the Kronecker channel model are 0.5 and 0.8.

The first outstanding observation is the increased gap between ZF and SOCP, compared to the simplified model in the previous sections. Figure 24 has a gap of 4dB even for 100 antennas. As explained before, ZF wastes some d.o.fs for eliminating the inter-

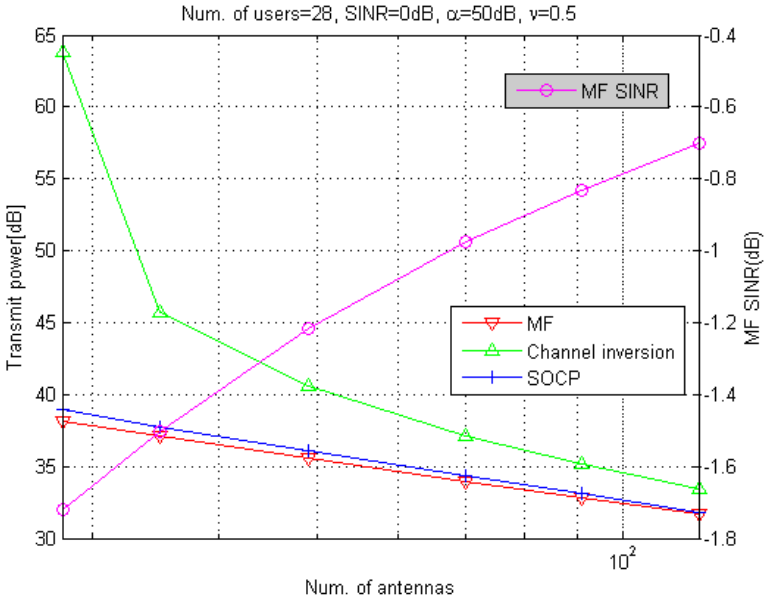

Figure 23: Transmit power versus num. of antennas, SINR= 0dB, $\nu = 0.5$.

ference towards the users with weak channels, which results in a performance gap with respect to the SOCP algorithm. This gap is bigger in the network simulation because the number of users in the network is more than the simplified model studied in the previous section, therefore designing an optimal beamformer becomes more critical. Increasing the target SINR decreases this gap that is due to the tendency of the SOCP algorithm to follow the ZF strategy when the target SINR increases, as discussed in Section 4.1 (for example, compare Figures 24 and 26).

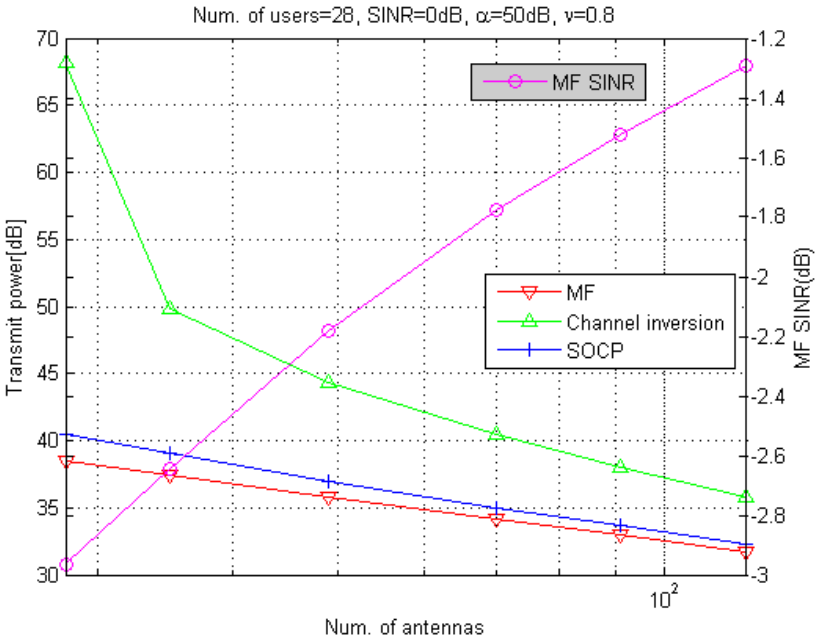

Figure 24: Transmit power versus num. of antennas, SINR= 0dB, $\nu = 0.8$.

The performance of the MF beamforming is also worse than the simplified model. The achieved SINR for the MF beamforming in Figure 24 is far from the target SINR.

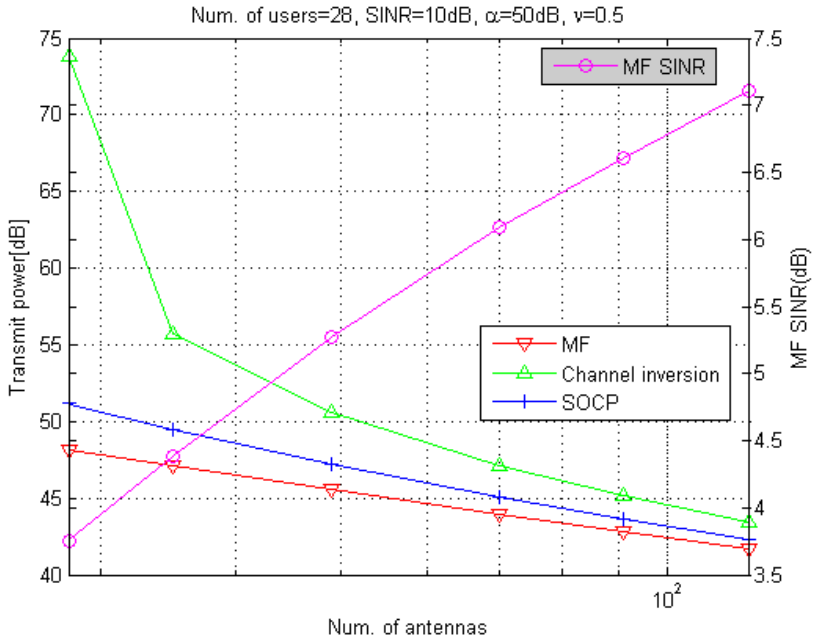

Figure 25: Transmit power versus num. of antennas, SINR= 10dB, $\nu = 0.5$.

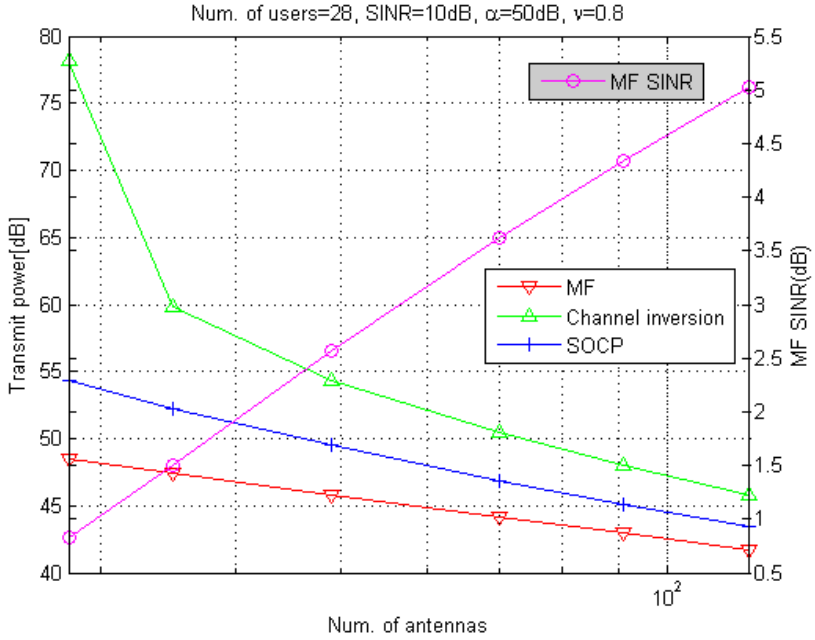

Figure 26: Transmit power versus num. of antennas, SINR= 10dB, $\nu = 0.8$.

In the above simulations, the number of antennas at BS is assumed more than 28 (the number of users in the network is 28) that guarantees the feasibility of ZF. Another interesting observation is related to the range of the number of antennas less than 28 which is depicted in Figure 27 for SINR=10dB. It can be seen that ZF becomes infeasible when the number of antennas at BS is less than 28, while the SOCP algorithm remains feasible even for the number of antennas less than number of users.

Until now, an effort has been made to understand the behavior of different algorithms in a realistic scenario, i.e when there is correlation between channel entries and users

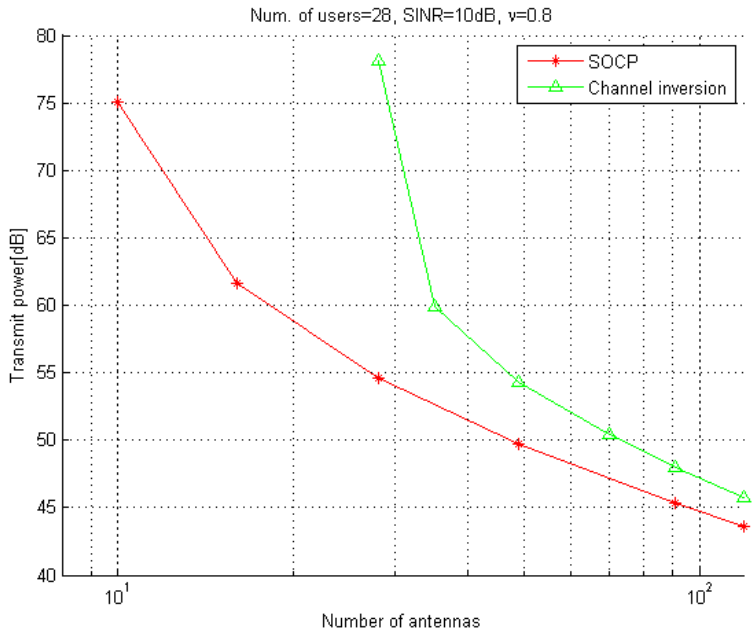

Figure 27: Infeasibility of ZF , SINR= 10dB, $\nu = 0.8$.

are scattered in a network. However, there are some other imperfections that are not considered here, such as imperfect CSI and hardware and non-ideal medium etc. Nevertheless, the network simulation shows that the gap between ZF and SOCP remained significant even for 100 antennas at base station. It must be noted that implementing more than 25 antennas per user (equivalent to 100 antennas at the base station in the network simulation) must be thought from a practical point of view. Moreover, the propagation medium puts another constraint on the number of d.o.fs available for each user. Thus, it can be concluded that the application of an optimal algorithm like SOCP seems beneficial even for a massive MIMO system.

4.3. Validity of large dimensions approximation based on simulation

In Section 3.4.2, the large dimensions behavior of the optimal intercell interference in the SOCP algorithm has been derived using random matrix theory. It has been shown that the optimal intercell interference of a system with large dimensions depends on channel statistics and not on instantaneous channel realization. The validity of this statement is examined in this section based on the simulation results.

The system model considered here is the same as in Section 4.2. The objective of this section is comparing the performance of the SOCP algorithm based on average and instantaneous intercell interference. In order to perform this comparison, the same simulation as Section 4.2 is repeated for a network with 28 users. The only difference is that the user's positions are fixed for all the trials. The simulation is performed for both of the instantaneous and the average intercell interferences.

In one simulation, the instantaneous optimal intercell interference is calculated for each channel realization, using which, the optimal transmit power is achieved, i.e,

the optimal power resulted from (21). Then, the optimal powers for all the channel realizations are averaged and stored for further analysis.

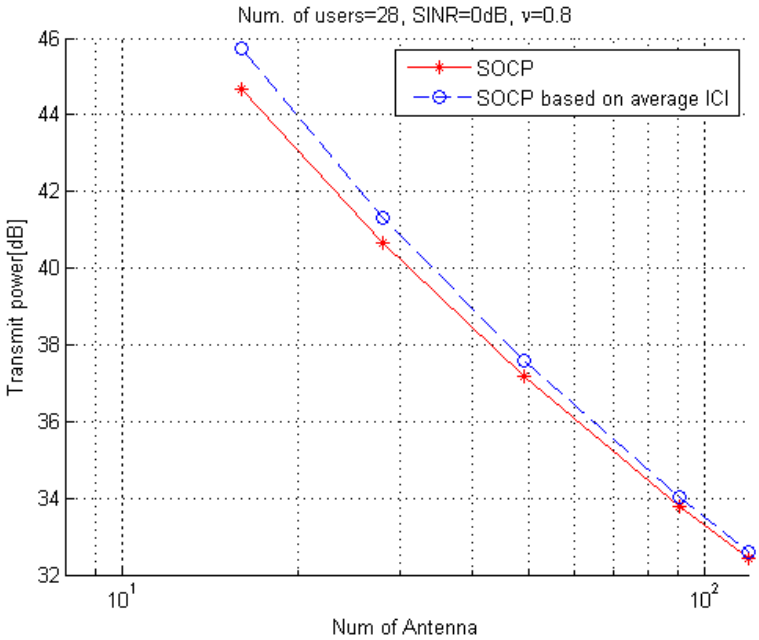

Figure 28: Transmit power versus num. of antennas, SINR= 0dB, $\nu = 0.8$.

The other simulation, use an average optimal intercell interference for all the channel realizations (instead of calculating the instantaneous optimal intercell interference for each channel realization). In other words, an average ϵ value is used in (27) for obtaining the optimal powers. The average optimal intercell interference is achieved by averaging the instantaneous optimal intercell interferences from the former simulation. The averaging of the instantaneous ICI makes the average optimal ICI independent of the channel realization which results an optimal ICI based on the channel statistics. The transmit powers for both of these simulations are depicted in Figures 28 and 29.

As can be seen from the figures, the transmit power based on the average ICI follows the instantaneous one with a gap; however, this gap is less than 2dB even when the number of antennas is small. Note that the other dimension of the problem, i.e the number of users is already 28, therefore, the average ICI provides a good approximation, even for the number of antennas equal to 16. Nevertheless, this gap gets smaller when the number of antennas grows larger.

Comparing Figures 28 and 29, it is can be inferred that the gap between curves gets smaller when the target SINR increases. This is due to the fact that a high target SINR causes the SOCP algorithm to follow a strategy like ZF, i.e an intercell interference equal to zero, thus the results based on the average and instantaneous ICI comes closer.

According to the results of this simulation, it can be concluded that the optimal intercell interference based on the channel statistics provides a good approximation, even for finite dimensions. Thus, the behaviors predicted by the approximations developed in Section 3.4.2 are valid. Therefore, these kind of approximations can be used for a practical scenario with limited dimensions.

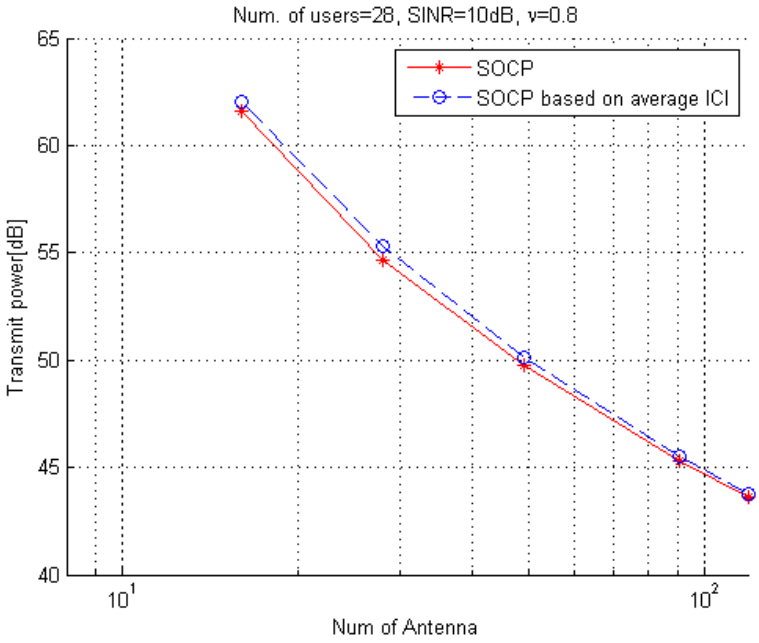

Figure 29: Transmit power versus num. of antennas, SINR= 10dB, $\nu = 0.8$.

4.4. Summary and discussion

The simulations in this chapter provide a general view about the performance of different methods with various number of antennas. It has been seen that for a practical scenario with antenna correlation and limited number of antennas, the SOCP algorithm performs better than ZF and MF. In the network simulation, the performance gap with respect to ZF has been noticeable, even for 120 antennas at the base stations.

In addition, the results of the simulation based on the average ICI have been in line with the behaviors predicted by the large dimension approximations in Section 3.4.2. Based on these results, it can be claimed that these kind of approximations are applicable to practical cases with limited dimensions.

5. DISCUSSION

The initial target of this study has been performance comparison between CoMP and other sub-optimal methods like the ZF and MF beamforming, when applied to a cellular network with large antenna arrays at base stations. The CoMP method considered here is minimum power beamforming. Two solutions have been reviewed for the minimum power beamforming problem, among which, the SOCP algorithm has been selected as the benchmark. The idea has been to see how much better CoMP can perform, compared to the simple sub-optimal methods, when the antenna array grows large.

The simulations show that under the ideal channel conditions, the performances of all the different methods converge, as the number of antennas grows large. This is not surprising, because it is already predicted by the theories. However, the rates of the convergence for different algorithms are not the same. The MF beamforming requires at least 30 d.o.f per user, in order to fulfill the target SINR to some acceptable level, while the ZF and SOCP algorithms satisfy the target SINR with much smaller number of d.o.f. Therefore, the MF beamforming can be considered as an inefficient method, even for the ideal channels. Nevertheless, the MF beamforming is simple, in a way that it allows distributed implementation of antenna array, which results in a performance improvement. However, the simulations do not take it into account.

Practical considerations put some constraints on the ultimate performance achievable by massive MIMO. One such restriction modeled in the simulations is correlation among antenna elements. The results show that increasing the inter antenna elements correlation demands a more efficient use of the available d.o.fs which result in a bigger gap between the SOCP and the ZF algorithms. For example, in the network simulation (with 7 BSs and 28 users) a gap of 4dB is observed even with 120 antennas at base stations. However, other imperfections such as: imperfect CSI and hardware, coupling among antenna elements and limitations on the number of d.o.f imposed by the propagation medium, etc are not considered. Perhaps, considering all of these issues brings a bigger performance gap between the SOCP algorithm and other sub-optimal methods. Nevertheless, the performance difference observed in the network simulation with correlation is big enough to motivate studying the large dimension behaviors of the SOCP algorithm.

The other parameters that are considered in the simulations are target SINR and user's distances. It is seen that a higher target SINR results in a smaller performance difference between the ZF and the SOCP algorithms. Moreover, the simplified simulation with 2 base stations (Section 4.1) shows that the SOCP algorithm for the users on the cell edges tends to follow a strategy like ZF. While for the users far from the cell edges, the ZF algorithm is far from being an efficient beamforming method. Another observation is related to the optimal user allocation. It is seen that for the users on the cell edges, there is a big gain resulted from the fast user allocation. This gain diminishes and becomes small as the number of antennas increases. However, even when the gap between the ZF and the SOCP algorithms disappears as a function of the number of antennas, the gap between the methods with and without the optimal BS assignment remains visible. The network simulation does not modeled the optimal BS assignment, thus, one might expect even a bigger gap due to the optimal BS assignment for the users

scattered on the cell boundaries of a network which indicates the gains in optimal user allocation strategies merged with distributed optimal beamfroming algorithms.

In Section 3.4.2 behavior of the SOCP algorithm with large dimensions is studied. The intercell interference term is considered as a parameter that affects both of the complexity and the backhaul exchange rate. Thus, by providing a large dimension approximation for this parameter, two goals are tackled. It is seen that this approximation is just a modification of the raw gauss given by $\alpha_{b,k}^2 \sum_{l \in \mathcal{U}_b} p_{b,l}$ with some other parameters, i.e, the uplink power and the Stieltjes transform of the channel matrix. All the parameters that contributes to the large dimension approximation of the optimal intercell interference, just depends on the channel statistics. Therefore, large dimensions inherently reduces the inter BSs exchange rates, because the channel statistics do not change very rapidly and an optimal ICI remains valid for several symbol times. Moreover, the prediction of the optimal ICI based on the channel statistics allowed proposal of a procedure for decoupling the subproblems at the base stations. According to this algorithm, the subproblems at the base stations can be solved independently when the optimal ICI is calculated based on the channel statistics. Finally, the simulations in Section 4.3 prove that the optimal powers resulted from the SOCP algorithm based on the average and the instantaneous ICI converges when the dimensions grow large, which is in line with the behavior predicted by the approximations.

Authors in [20] provide an algorithm for the minimum power beamforming with large dimensions based on the concepts of uplink-downlink duality. This procedure translates the error in approximation to a difference between the resulted and target SINRs. Thus, the target SINR cannot be guaranteed using this algorithm. Unlike this method, the approximations for the SOCP solution did not affect the resulted SINR, but causes a higher transmit power. Generally, it is desired to fulfill user's quality of service, even with a higher transmit power. Thus, the performance of the approximations based on the SOCP solution seems more favorable. However, the algorithm developed by [20] is easier to be implemented. Nevertheless, the initial goal of the thesis has not been proposing a practical algorithm, but the characterizations of the SOCP algorithm at large dimensions regime pave the way towards a practical algorithm based on the SOCP solution

The approximations for the minimum power beamforming developed in this thesis work can be applied to a cellular network with large dimensions. The dimensions of the problem consist of the number of antennas at BS and the number of users in the network. It is already seen in the simulations that the approximations are valid for the dimensions as big as 30 (or even less, depending on the tolerable error). Thus, the results can be applied to the problems with practical finite dimensions. Massive MIMO is one such problem that can be tackled efficiently by using these approximations. In addition to the ordinary networks with users as the service nodes, other scenarios like the one suggested by work in [40] can be considered for application of the approximations developed here. Authors in [40] suggest a scenario where a coverage area is served by a macro base station with a large antenna array and several small cell single antenna base stations. They suggest that on demand wireless backhaul links for these small cells can be provided by the macro base station (that has a large antenna array). Thus, a beamforming method like the SOCP algorithm can be used for delivering the services to these small cell base stations. The channel statistics in this scenario do not

change very rapidly (due to the fixed positions of nodes) which makes the realtime deployment of the SOCP algorithm easier.

According to the results, it can be concluded that the performance gap between the optimal and sub-optimal beamforming methods under realistic assumptions is big enough to motivate the development of optimal methods for large dimension problems. The large dimension approximations reduce the complexity of such algorithms and the error due to the approximations seems tolerable for practically finite dimensions. Moreover, these simplifications allow the application of the algorithms that might have not been considered before, due to the complexity and real-time restrictions. The SOCP algorithm as one such method is considered in this thesis work and the large dimension behavior characterizations developed here pave the way for proposing a practical method based on this solution.

6. SUMMARY

The goal defined for this study is comparing the performance of minimum power beamforming, as an optimal method, with some sub-optimal methods such as: ZF and MF beamforming, when dimensions grow large. Two solutions for the minimum power beamforming are reviewed, among which, the SOCP algorithm is selected as the benchmark.

According to theories, under an ideal scenario, performances of all the methods converge as the number of antennas grows large. However, this is not generally true when practical considerations are taken into account. In the network simulation with 7 BS and 28 users, it is seen that the inter antenna elements correlation causes a significant gap between the optimal and suboptimal methods even with 100 antennas at BS. Generally, a higher correlation among the antenna elements causes a bigger performance gap. Therefore, under realistic assumptions a more efficient use of resources are required which justifies the efforts in characterizing the behavior of the SOCP algorithm with large dimensions.

Intercell interference (ICI) is a key parameter in the SOCP algorithm that couples the sub-problems at base stations. Thus, a large dimension approximation for this parameter is derived that allows characterization of the SOCP algorithm in large dimensions regime. This approximation shows that the optimal ICI just depends on statistics of channel which indicates a smaller backhaul exchange rate requirement in the large dimension regime. According to the predictable behavior of the optimal ICI based on the channel statistics, a procedure is proposed for decoupling the subproblems at base stations which results in the processing simplification. The simulation proves that the error due to the approximations disappears as the dimensions grow large. These results lead the way towards proposing a practical algorithm based on the SOCP solution for a problem with large dimensions.

Generally, it can be concluded that under realistic assumptions, an efficient use of the resources can bring a significant performance improvement for a cellular network with practically large antenna array. This goal can be fulfilled by applying optimal algorithms such as SOCP. The complexity of such solutions for a problem with large dimensions can be dealt by simplification resulted from large dimensions approximations.

7. REFERENCES

[1] E. Dahlman S. Parkvall J.S. & Beming P. (2008) 3G Evolution HSPA and LTE for Mobile Broadband. Academic Press, first ed.

[2] Boccardi F., Clerckx B., Ghosh A., Hardouin E., Jongren G., Kusume K., Onggosanusi E. & Tang Y. (2012) Multiple-antenna techniques in lte-advanced. IEEE Communications Magazine 50, pp. 114–121.

[3] Tse D. & Viswanat P. (2005) Fundamentals of Wireless Communication. Cambridge University Press, first ed.

[4] Rusek F., Persson D., Lau B.K., Larsson E.G., Marzetta T.L., Edfors O. & Tufvesson F. (2013) Scaling up mimo: Opportunities and challenges with very large arrays. IEEE Signal Processing Magazine 30, pp. 40–60. ID: 1.

[5] Marzetta T.L. (2010) Noncooperative cellular wireless with unlimited numbers of base station antennas. IEEE Transactions on Wireless Communications 9, pp. 3590–3600.

[6] Romain Couillet M.D. (2011) Random Matrix Methods for Wireless Communications. First ed.

[7] Gao X., Edfors O., Rusek F. & Tufvesson F. (2011) Linear pre-coding performance in measured very-large mimo channels. In: Vehicular Technology Conference (VTC Fall), IEEE, pp. 1–5.

[8] Hoydis J., Hoek C., Wild T. & ten Brink S. (2012) Channel measurements for large antenna arrays. In: International Symposium on Wireless Communication Systems (ISWCS), IEEE, pp. 811–815.

[9] Karakayali M., Foschini G.J., Valenzuela R.A. & Yates R.D. (2006) On the maximum common rate achievable in a coordinated network. In: IEEE International Conference on Communications, ICC'06., vol. 9, IEEE, vol. 9, pp. 4333–4338.

[10] Schubert M. & Boche H. (2004) Solution of the multiuser downlink beamforming problem with individual sinr constraints. IEEE Transactions on Vehicular Technology 53, pp. 18–28.

[11] Bengtsson M. & Ottersten B. (2001) Optimal and suboptimal transmit beamforming .

[12] Venkatesan S., Lozano A. & Valenzuela R. (2007) Network mimo: Overcoming intercell interference in indoor wireless systems. In: Conference Record of the Forty-First Asilomar Conference on Signals, Systems and Computers, IEEE, pp. 83–87.

[13] Irmer R., Droste H., Marsch P., Grieger M., Fettweis G., Brueck S., Mayer H.P., Thiele L. & Jungnickel V. (2011) Coordinated multipoint: Concepts, performance, and field trial results. IEEE Communications Magazine 49, pp. 102–111.

[14] Gao Y., Li Y., Yu H. & Gao S. (2011) Performance of dynamic comp cell selection in 3gpp lte system level simulation. In: IEEE 3rd International Conference on Communication Software and Networks (ICCSN), IEEE, pp. 210–213.

[15] Venturino L., Prasad N. & Wang X. (2009) Coordinated scheduling and power allocation in downlink multicell ofdma networks. IEEE Transactions on Vehicular Technology 58, pp. 2835–2848.

[16] Yu W. & Lan T. (2007) Transmitter optimization for the multi-antenna downlink with per-antenna power constraints. IEEE Transactions on Signal Processing 55, pp. 2646–2660.

[17] Dahrouj H. & Yu W. (2010) Coordinated beamforming for the multicell multi-antenna wireless system. IEEE Transactions on Wireless Communications 9, pp. 1748–1759.

[18] Bengtsson M. & Ottersten B. (1999) Optimal downlink beamforming using semidefinite optimization. In: Proceedings of the Annual Allerton Conference on Communication Control and Computing, vol. 37, Citeseer, vol. 37, pp. 987–996.

[19] Tolli A., Pennanen H. & Komulainen P. (2011) Decentralized minimum power multi-cell beamforming with limited backhaul signaling. IEEE Transactions on Wireless Communications 10, pp. 570–580.

[20] Lakshminaryana S., Hoydis J., Debbah M. & Assaad M. (2010) Asymptotic analysis of distributed multi-cell beamforming. In: 21st IEEE nternational Symposium on Personal Indoor and Mobile Radio Communications (PIMRC), pp. 2105–2110.

[21] Nam J., Ahn J.Y., Adhikary A. & Caire G. (2012) Joint spatial division and multiplexing: Realizing massive mimo gains with limited channel state information. In: 46th Annual Conference on Information Sciences and Systems (CISS), pp. 1–6.

[22] Shepard C., Yu H., Anand N., Li E., Marzetta T., Yang R. & Zhong L. (2012) Argos: practical many-antenna base stations. In: Proceedings of the 18th annual international conference on Mobile computing and networking, Mobicom '12, ACM, New York, NY, USA, pp. 53–64. URL: http://doi.acm.org/10.1145/2348543.2348553.

[23] Hoydis J., ten Brink S. & Debbah M. (2011) Massive mimo: How many antennas do we need? In: 49th Annual Allerton Conference on Communication, Control, and Computing (Allerton), pp. 545–550. ID: 1.

[24] Kay S.M. (1993) Fundamentals of statistical signal processing, volume i: Estimation theory (v. 1) .

[25] Ngo H.Q., Larsson E. & Marzetta T. (2013) Energy and spectral efficiency of very large multiuser mimo systems. IEEE Transactions on Communications 61, pp. 1436–1449.

[26] Ngo H.Q. & Larsson E. (2012) Evd-based channel estimation in multicell multiuser mimo systems with very large antenna arrays. In: IEEE International Conference on Acoustics, Speech and Signal Processing (ICASSP), pp. 3249–3252.

[27] Appaiah K., Ashikhmin A. & Marzetta T. (2010) Pilot contamination reduction in multi-user tdd systems. In: IEEE International Conference on Communications (ICC), pp. 1–5.

[28] Jose J., Ashikhmin A., Marzetta T. & Vishwanath S. (2011) Pilot contamination and precoding in multi-cell tdd systems. IEEE Transactions on Wireless Communications 10, pp. 2640–2651.

[29] Ashikhmin A. & Marzetta T. (2012) Pilot contamination precoding in multi-cell large scale antenna systems. In: IEEE International Symposium on Information Theory Proceedings (ISIT), pp. 1137–1141.

[30] Yin H., Gesbert D., Filippou M. & Liu Y. (2013) A coordinated approach to channel estimation in large-scale multiple-antenna systems. IEEE Journal on Selected Areas in Communications 31, pp. 264–273.

[31] E. Bjornson J. Hoydis M.K. & Debbah M. Hardware impairments in large-scale miso systems: Energy efficiency, estimation, and capacity limits. Proc. International Conference on Signal Processing (DSP) .

[32] Alain Sibille Claude Oestges A.Z. (2010) MIMO: From Theory to Implementation. First ed.

[33] Correia L.M. (2006) Mobile Broadband Multimedia Networks: Techniques, Models and Tools for 4G. First ed.

[34] Stephen Boyd L.X. & Mutapcic A. (2003) Notes on decomposition methods. Notes for EE392o, Stanford University, Autumn, 2003 .

[35] Pennanen H., Tolli A. & Latva-Aho M. (2011) Decentralized coordinated downlink beamforming via primal decomposition. IEEE Signal Processing Letters 18, pp. 647–650.

[36] Shen C., Chang T.H., Wang K.Y., Qiu Z. & Chi C.Y. (2012) Distributed robust multicell coordinated beamforming with imperfect csi: An admm approach. IEEE Transactions on Signal Processing 60, pp. 2988–3003.

[37] M. Chiang P. Hande T.L.C.T. (2006) Power control in Wireless Cellular Networks. First ed.

[38] Kaare Brandt Petersen M.S.P. (2012) The Matrix Cookbook. First ed.

[39] Kermoal J., Schumacher L., Pedersen K., Mogensen P. & Frederiksen F. (2002) A stochastic mimo radio channel model with experimental validation. IEEE Journal on Selected Areas in Communications 20, pp. 1211–1226.

[40] Hoydis J. (2013) Massive mimo and hetnets: Benefits and challenges. Interference Management for Tomorrow's Wireless Networks, Eurecom Sophia-Antipolis France .

[41] Walid Hachem P.L. & Najim J. (2007) Deterministic equivalents for certain functionals of large random matrices. Ann. Appl. Probab. Volume 17, Number 3 .

[42] J.W. Silverstein Z.B. (1995) On the empirical distribution of eigenvalues of a class of large dimensional random matrices. Journal of Multivariate Analysis .

[43] J.W. Silverstein Z.B. (1998) No eigenvalues outside the support of the limiting spectral distribution of large dimensional sample covariance matrices. Annals of probability .

8. APPENDICES

A. Random matrix theory

This appendix is dedicated to an overview about RMT. Some lemmas and theories are presented which are used throughout the thesis. For more details refer to [6].

At first, a useful tool, known as Stieltjes transform is introduced which simplifies the derivation of theorems in RMT field. Stieltjes transform is defined as follows,

Definition A-1. [6], Assuming a real valued bounded measurable function over $\mathbb{R}$ denoted by F, the Stieltjes transform of F for $z \in Supp(F)^c$ is defined as:

$$m_F(z) = \int_{-\infty}^{\infty} \frac{1}{\lambda - z} dF(\lambda) \tag{60}$$

The Stieltjes transform has inverse defined by the following theorem.

Theorem A-1. [6], Assuming x to be a continuity point of F then,

$$F(x) = \frac{1}{\pi} lim_{t \to 0^+} \int_{-\infty}^{x} \Im[m_F(x + it)] dx \tag{61}$$

F can be any function that satisfies the specified condition in Definition A-1. However, for studies here, F is a distribution function. For a distribution function F, it can be shown that the Stieltjes transform uniquely defines F and vice versa [6]. A special distribution function is the empirical spectral distribution (e.s.d.) of a $N \times N$ Hermitian matrix $\mathbf{Y}_N$, defined as follows,

Definition A-2. [6], $F(x)$ is assumed to be empirical spectral distribution(e.s.d.) of $\mathbf{Y}_N$, where $\mathbf{Y}_N$ is a $N \times N$ Hermitian matrix and $x \in \mathbb{R}$ then,

$$F(x) = \frac{1}{N} \sum_{j=1}^{N} 1_{\lambda_j \leq x}(x) \tag{62}$$

Where $\lambda_1, ..., \lambda_N$ are eigenvalues of $\mathbf{Y}_N$. $1_{\lambda_j \leq x}$ is a function which gives 1 when λ_j is less than x.

The use of Stieltjes transform for simplifying the analysis of eigenvalue distribution of large dimension matrices might not be clear yet. Thus, the following lemma is introduced which makes the Stieltjes transform attractive.

Lemma A-1. [6],For a Hermitian matrix $\mathbf{Y}$:

$$m_F(z) = \int \frac{1}{\lambda - z} dF(\lambda) \tag{63}$$

$$= \frac{1}{N} tr(\mathbf{\Lambda} - z\mathbf{I}_N)^{-1} \tag{64}$$

$$= \frac{1}{N} tr(\mathbf{Y} - z\mathbf{I}_N)^{-1} \tag{65}$$

From the above lemmas, two points can be inferred. First, it is known that when all the moments of a probability distribution function are available, it is possible to

reconstruct the probability distribution function (p.d.f) based on its moments. Looking at (62) and (63), one can show that Stieltjes transform is a one shot transform from p.d.f to its moments. Second, the above lemma simplifies the calculation of the Stieltjes transform. In other words, the Stieltjes transform can be achieved by summing up the diagonal elements of $(\mathbf{Y} - z\mathbf{I}_{\mathrm{N}})^{-1}$. These properties make the Stieltjes transform attractive for problem analysis in large dimension domain.

The above theorems and lemmas provide tools that are used for driving Stieltjes transform of different matrices. One of such matrices that is of particular interest is Gram matrix. Gram matrix related to any matrix $\mathbf{X}$ is defined as $\mathbf{X}\mathbf{X}^H$. This structure appears in the signal processing topics. Here one such Gram matrix is considered and following theorem gives the equations for deriving its Stieltjes transform.

Theorem A-2. [20] [41], Consider a $N \times n$ random matrix denoted by $\mathbf{Y}$, such that elements of $\mathbf{Y}$ are independent and zero mean. The variance of entries is given by $E[|y_{i,j}|^2] = \alpha_{i,j}^2$ which are uniformly bounded from above. Also some soft restrictions are assumed over higher moments. then,

$$\frac{1}{N}tr(\mathbf{Y}\mathbf{Y}^H - z\mathbf{I}_{\mathrm{N}})^{-1} - \frac{1}{N}tr(\mathbf{\Theta}(z)) \xrightarrow{n \to \infty,\, \frac{N}{n} \to c} 0, \forall z \in \mathbb{C} - \mathbb{R}^+ \tag{66}$$

Where $\mathbf{\Theta}(z) = diag(\theta_1(z), ..., \theta_N(z))$ is a deterministic matrix valued function, analytic in $\mathbb{C} - \mathbb{R}^+$. The entries of this function can be found by initializing and iterating the following system of $N + n$ equations:

$$\theta_i(z) = \frac{-1}{z(1 + \frac{1}{n}\sum_{j=1}^{n} \alpha_{i,j}^2 \hat{\theta}_j(z))} \forall 1 \leq i \leq N \tag{67}$$

$$\hat{\theta}_j(z) = \frac{-1}{z(1 + \frac{1}{n}\sum_{i=1}^{N} \alpha_{i,j}^2 \theta_i(z))} \forall 1 \leq j \leq n \tag{68}$$

It is also sometimes required to calculate the derivative of Stieltjes transform of the matrix $\mathbf{Y}\mathbf{Y}^H$. This derivative is given by $\frac{1}{N}tr(\mathbf{\Theta}'(z))$. Where $\mathbf{\Theta}'(z) = diag(\theta_1'(z), ..., \theta_N'(z))$. The entries can be found by solving a system of equation resulted from taking derivatives of (67) and (68) with respect to z [20].

In addition to the above theorems and lemmas there are some other lemmas that are important for derivation of large dimension approximations which are presented as follows,

Lemma A-2.[42]: Assume $\mathbf{A}$ to be a $N \times N$ Hermitian invertible matrix, then $\mathbf{A} + \nu\mathbf{x}\mathbf{x}^H$, where $\mathbf{x} \in \mathbb{C}^N, \nu \in \mathbb{C}$, is invertible and its inverse is given by,

$$x^H(\mathbf{A} + \nu\mathbf{x}\mathbf{x}^H)^{-1} = \frac{\mathbf{x}^H\mathbf{A}^{-1}}{1 + \nu\mathbf{x}^H\mathbf{A}^{-1}\mathbf{x}} \tag{69}$$

Lemma A-3. [43]: Assume a vector $\mathbf{x} \in \mathbb{C}^N$ with i.i.d elements which have zero mean and variance equal to $\frac{1}{N}$. Also consider a Hermitian matrix $\mathbf{A} \in \mathbb{C}^{N \times N}$ with elements independent of $\mathbf{x}$ and $limSup_N||\mathbf{A}|| < \infty$, then:

$$\mathbf{x}^H\mathbf{A}\mathbf{x} - \frac{1}{N}tr(\mathbf{A}) \xrightarrow{a.s.} 0 \tag{70}$$

Lemma A-4.(Rank-1 perturbation lemma) [42] let **A** and **B** to be $N \times N$ matrices. **B** is also conditioned to be Hermitian and nonnegative definite. Also there is $Z \in \mathbb{C}\backslash\mathbb{R}^{+}$ and $\nu = dist(z, \mathbb{R}^{+})$, where $dist$ indicates the Euclidean distance between the entries, $\tau \in \mathbb{R}$ and $\mathbf{x} \in \mathbb{C}^{N}$ then,

$$|tr[(\mathbf{B} - z\mathbf{I})^{-1} - (\mathbf{B} + \tau\mathbf{x}\mathbf{x}^{H} - z\mathbf{I})^{-1}]\mathbf{A}| \leq \frac{||\mathbf{A}||}{\nu} \tag{71}$$

Where, $||\mathbf{A}||$ indicates the spectral norm of the matrix **A**

In this appendix a review over some fundamental results from random matrix theory have been presented which are used throughout the thesis for derivation and explanation of large dimension approximations. For further information about random matrix theory refer to the work in [6] .